UNITED NATIONS UNIVERSITY

UNU-GTP

Geothermal Training Programme

ORKUSTOFNUN

Blési hot spring at Geysir geothermal field

Malcolm Grant

LECTURES ON GEOTHERMAL RESERVOIR ENGINEERING

Report 4
December 2014

UNITED NATIONS UNIVERSITY
UNU-GTP
Geothermal Training Programme

GEOTHERMAL TRAINING PROGRAMME
Orkustofnun, Grensasvegur 9,
IS-108 Reykjavik, Iceland

Reports 2014
Number 4

LECTURES ON GEOTHERMAL RESERVOIR ENGINEERING

Malcolm Grant
208D Runciman Rd
RD2, Pukekohe 2677
NEW ZEALAND
malcolm@grant.net.nz

Lectures given in August 2014
United Nations University Geothermal Training Programme
Reykjavik, Iceland
Published in December 2014

ISBN 978-9979-68-343-8
ISSN 1670-7400

PREFACE

The visiting lecturer of UNU 2014 is the reservoir engineer Dr. Malcolm Grant from New Zealand. Dr. Grant holds a doctoral degree in applied mathematics from MIT. In 1973, he joined the DSIR and began working as a geothermal reservoir engineer. He was the Geothermal Coordinator for the DSIR in 1985-1987. From 1988 to 1991, he was the general manager of the New Zealand Meteorological Service, and in 1992-1994, he was the chief executive of NIWA. He has been involved in various research and management projects and has worked as a private consultant since 1994. He has been involved in assessment and development of 76 geothermal fields in 14 countries.

Dr. Grant was awarded the New Zealand 1990 Commemoration Medal, and the 2010 Henry J. Ramey Geothermal Reservoir Engineering Award from the Geothermal Resources Council.

Dr. Grant is among the most prestigious scientists in the field of geothermal and has published many papers on reservoir engineering. He is the senior author of the widely used textbook *Geothermal Reservoir Engineering*.

Since the foundation of the UNU-GTP in 1979, it has been customary to invite annually one internationally renowned geothermal expert to come to Iceland as the UNU Visiting Lecturer. This has been in addition to various foreign lecturers who have given lectures at the Training Programme from year to year. It is the good fortune of the UNU Geothermal Training Programme that so many distinguished geothermal specialists have found time to visit us. Following is a list of the UNU Visiting Lecturers during 1979-2013:

1979 Donald E. White	United States	1997 Toshihiro Uchida	Japan 1980
Christopher Armstead	United Kingdom	1998 Agnes G. Reyes	Philippines/N.Z.
1981 Derek H. Freeston	New Zealand	1999 Philip M. Wright	United States
1982 Stanley H. Ward	United States	2000 Trevor M. Hunt	New Zealand
1983 Patrick Browne	New Zealand	2001 Hilel Legmann	Israel
1984 Enrico Barbier	Italy	2002 Karsten Pruess	United States
1985 Bernardo Tolentino	Philippines	2003 Beata Kepinska	Poland
1986 C. Russel James	New Zealand	2004 Peter Seibt	Germany
1987 Robert Harrison	United Kingdom	2005 Martin N. Mwangi	Kenya
1988 Robert O. Fournier	United States	2006 Hagen M. Hole	New Zealand
1989 Peter Ottlik	Hungary	2007 José Antonio Rodríguez	El Salvador
1990 Andre Menjoz	France	2008 Wang Kun	China
1991 Wang Ji-yang	China	2009 Wilfred A. Elders	United States
1992 Patrick Muffler	United States	2010 Roland N. Horne	United States
1993 Zosimo F. Sarmiento	Philippines	2011 Ernst Huenges	Germany
1994 Ladislaus Rybach	Switzerland	2012 Cornel Ofwona	Kenya
1995 Gudmundur Bödvarsson	United States	2013 Kevin Brown	New Zealand
1996 John Lund	United States		

With warmest greetings from Iceland

Lúdvík S. Georgsson, director, UNU-GTP

TABLE OF CONTENTS

Page

Page

LIST OF FIGURES

Page

LIST OF TABLES

UNITED NATIONS UNIVERSITY
UNU-GTP
Geothermal Training Programme

GEOTHERMAL TRAINING PROGRAMME
Orkustofnun, Grensasvegur 9,
IS-108 Reykjavik, Iceland

Reports 2014
Number 4

LECTURES ON GEOTHERMAL RESERVOIR ENGINEERING

Malcolm Grant
208D Runciman Rd
RD2, Pukekohe 2677
NEW ZEALAND
malcolm@grant.net.nz

Lectures given in August 2014
United Nations University Geothermal Training Programme
Reykjavik, Iceland
Published in December 2014

ISBN 978-9979-68-343-8
ISSN 1670-7400

PREFACE

The visiting lecturer of UNU 2014 is the reservoir engineer Dr. Malcolm Grant from New Zealand. Dr. Grant holds a doctoral degree in applied mathematics from MIT. In 1973, he joined the DSIR and began working as a geothermal reservoir engineer. He was the Geothermal Coordinator for the DSIR in 1985-1987. From 1988 to 1991, he was the general manager of the New Zealand Meteorological Service, and in 1992-1994, he was the chief executive of NIWA. He has been involved in various research and management projects and has worked as a private consultant since 1994. He has been involved in assessment and development of 76 geothermal fields in 14 countries.

Dr. Grant was awarded the New Zealand 1990 Commemoration Medal, and the 2010 Henry J. Ramey Geothermal Reservoir Engineering Award from the Geothermal Resources Council.

Dr. Grant is among the most prestigious scientists in the field of geothermal and has published many papers on reservoir engineering. He is the senior author of the widely used textbook *Geothermal Reservoir Engineering*.

Since the foundation of the UNU-GTP in 1979, it has been customary to invite annually one internationally renowned geothermal expert to come to Iceland as the UNU Visiting Lecturer. This has been in addition to various foreign lecturers who have given lectures at the Training Programme from year to year. It is the good fortune of the UNU Geothermal Training Programme that so many distinguished geothermal specialists have found time to visit us. Following is a list of the UNU Visiting Lecturers during 1979-2013:

1979 Donald E. White	United States	1997 Toshihiro Uchida	Japan 1980
Christopher Armstead	United Kingdom	1998 Agnes G. Reyes	Philippines/N.Z.
1981 Derek H. Freeston	New Zealand	1999 Philip M. Wright	United States
1982 Stanley H. Ward	United States	2000 Trevor M. Hunt	New Zealand
1983 Patrick Browne	New Zealand	2001 Hilel Legmann	Israel
1984 Enrico Barbier	Italy	2002 Karsten Pruess	United States
1985 Bernardo Tolentino	Philippines	2003 Beata Kepinska	Poland
1986 C. Russel James	New Zealand	2004 Peter Seibt	Germany
1987 Robert Harrison	United Kingdom	2005 Martin N. Mwangi	Kenya
1988 Robert O. Fournier	United States	2006 Hagen M. Hole	New Zealand
1989 Peter Ottlik	Hungary	2007 José Antonio Rodríguez	El Salvador
1990 Andre Menjoz	France	2008 Wang Kun	China
1991 Wang Ji-yang	China	2009 Wilfred A. Elders	United States
1992 Patrick Muffler	United States	2010 Roland N. Horne	United States
1993 Zosimo F. Sarmiento	Philippines	2011 Ernst Huenges	Germany
1994 Ladislaus Rybach	Switzerland	2012 Cornel Ofwona	Kenya
1995 Gudmundur Bödvarsson	United States	2013 Kevin Brown	New Zealand
1996 John Lund	United States		

With warmest greetings from Iceland

Lúdvík S. Georgsson, director, UNU-GTP

TABLE OF CONTENTS

Page

Page

LIST OF FIGURES

Page

LIST OF TABLES

LECTURE 1

INTERPRETATION OF DOWNHOLE MEASUREMENTS

1. INTRODUCTION

This chapter leads into the following sections on well testing and measurement, and introduces the distinctive problems in the interpretation of measurements made in a geothermal well. In other disciplines, petroleum and groundwater, running a pressure-temperature survey in a well usually results in straightforward data: In geothermal it usually does not. This section introduces downhole temperature and pressure measurements and their interpretation, production testing, test design and reporting.

In most cases it is not possible to directly measure the downhole characteristics that are needed to assess a geothermal resource. Indeed, measurements can on occasion be quite misleading, as shown in the following examples.

1.1 Temperatures in well WK10, Wairakei

This example shows an extreme case of the difference between measurements in the well and the state of the reservoir. WK10 was a peripheral shallow well at Wairakei, drilled in 1951. Figure 1 shows temperature profiles measured over a period of 20 years.

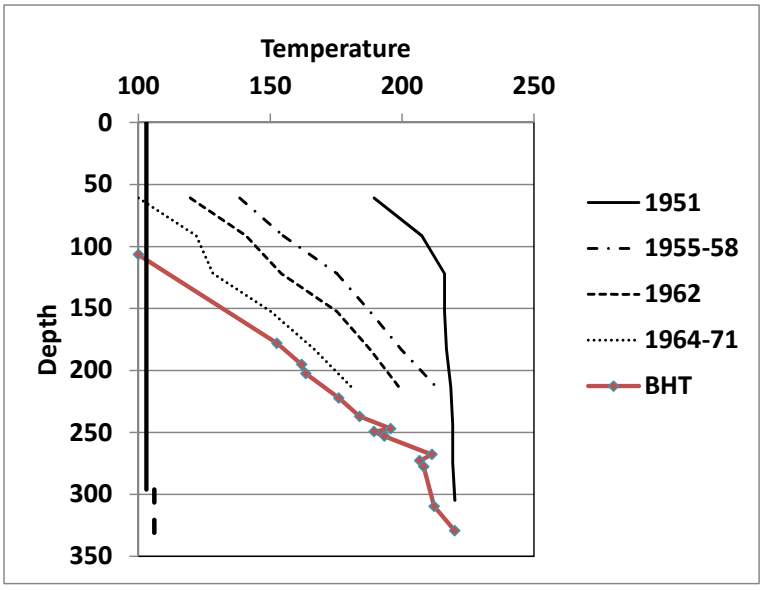

FIGURE 1: Temperatures in WK10

The successive measurements show an apparently clear history: temperature has declined steadily over time. As the well is on the edge of the field, this is not surprising, and it seems that it is showing the steady inflow of cooler waters from the field edge. However this is quite wrong. The bottomhole temperatures were measured during drilling (marked as "BHT" in Figure 1). Drilling was done only during daylight hours and the bottomhole temperature measured each day after approximately 12 hours heating overnight. These measurements should be close to the true formation temperature, as the bottom of the hole has been subjected to little circulation to cool the formation. The drilling reports also make it clear that the formation conditions were relatively cool before encountering hot and gassy conditions at 250m. The downhole profile in 1951 shows much hotter fluid in the well, except at well bottom. What is happening in 1951 is that hot fluid is flowing up the well from near well bottom, and exiting between 100 and 150m (presumably at a casing break). With time reservoir pressure falls due to exploitation, and the upflow weakens. Conductive heat losses become more important as the upflow decreases. Eventually by 1971 the measured temperatures are close to the original drilling bottomhole temperatures. Thus, the steady fall in measured temperature with time does not reflect a change in formation temperature outside the wellbore – the formation temperature did not change. Rather the change in temperature reflects a fall in pressure driving the upflow in the well.

1.2 Liquid-gas-liquid profile

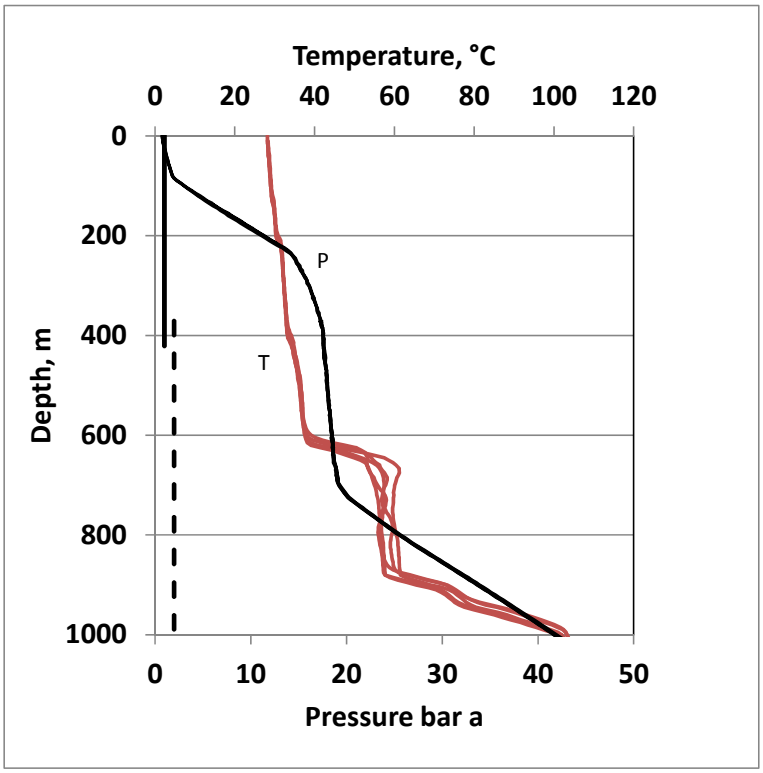

FIGURE 2: Water above steam in wellbore

Figure 2 shows a pressure-temperature profile which appears to have a vapour section between two liquid sections. Profiles of this form are encountered occasionally, usually in vapour-dominated reservoirs or steam zones, while injecting cold water. In this case the well is under injection at 40 kg/s and four passes were made using a PTS instrument: two up and two down. For all of these passes the profile remains essentially unchanged. The data shows that inside the perforated liner there is a gas zone sandwiched between liquid zones, above and below. In this case the reservoir has a segregated steam zone above a liquid zone and in this well there is a feed at 600m in the steam zone – indicated by the temperature increase during injection at this depth. During injection steam and gas are flowing into the wellbore. Steam is condensed leaving the gas which forms a bubble inside the perforated liner forcing the injected water to flow down around the liner annulus – the casing diagram shows the top of the bubble is just above the top of the perforated liner. The spinner data in the gas interval were very noisy; indicating some of the water was also showering down the inside of the perforated liner. Below 700m water is flowing down the well to a loss zone just above 900m. Within the casing the pressure gradient is near hydrostatic, or less than hydrostatic. This reflects the counterflow in the casing, water descending while gas bubbles rise to surface. In this case an unusual pressure profile can be explained by considering the fluids in the reservoir, the fluids in the wellbore, the feedzone depths and the configuration of the casing and perforated liner

1.3 Water level in a steam well

Figure 3 shows profiles in well DRJ-27 in the vapour-dominated field of Darajat, Indonesia. These results are fairly typical. Note the water level near well bottom. Does it represent a water level in the reservoir – no, other wells all show different water levels. Nor is it water accumulated in a dead leg, the temperatures show there is some fluid flow in the water. I will come back to this type of profile later.

So, often (or usually) the reservoir parameters are not directly measured by downhole profiles. Instead, an interpretation or inference is made from the information that is available from the well test programme. Interpretation of well test data involves bringing together a range of information from the drilling operations, geology, downhole measurements and production tests. Knowledge of other nearby well characteristics is also useful. Often the set of test data that is available will be incomplete, there may be errors in the measurements, or the well conditions may not be stable. The end result of these factors is that interpretation of well test data is an imperfect science. Different interpretations can be derived using the same data, and within the limitations of the available data both may be "correct". The reason for this is due to a combination of physical factors: the permeability distribution; the state of the reservoir; and the well design. In most geothermal reservoirs the permeability is not constrained within a uniform aquifer but is distributed as an array of fractures, varyingly pervasive through the rock, which

intersect the well at a few (almost random) points; the wellbore usually has an open hole section of up to 2000m; and the reservoir fluid is not static.

The consequences can be seen by considering a simple example: an exploration well drilled into the central upflow of a geothermal field. This well has permeability at a few depths, scattered along the open hole section. Outside the well there is a distribution of pressure *P(z)* and temperature *T(z)* with depth. The geothermal field has a natural flow rising from depth eventually reaching surface to discharge as springs and thermal features. For example, Figure 9 shows the distribution of pressure with depth in the centre of Mak-Ban. There is a vertical pressure gradient of 8.2 bar/100m, compared to hydrostatic (for the temperature) of about 7.4 bar/100m. Darcy's Law gives for the vertical flow density v_z:

$$v_z = \frac{k}{\mu}\left(\frac{dP}{dz} - \rho g\right)$$

or

$$\frac{dP}{dz} = \rho g + \frac{\mu}{k} v_z$$

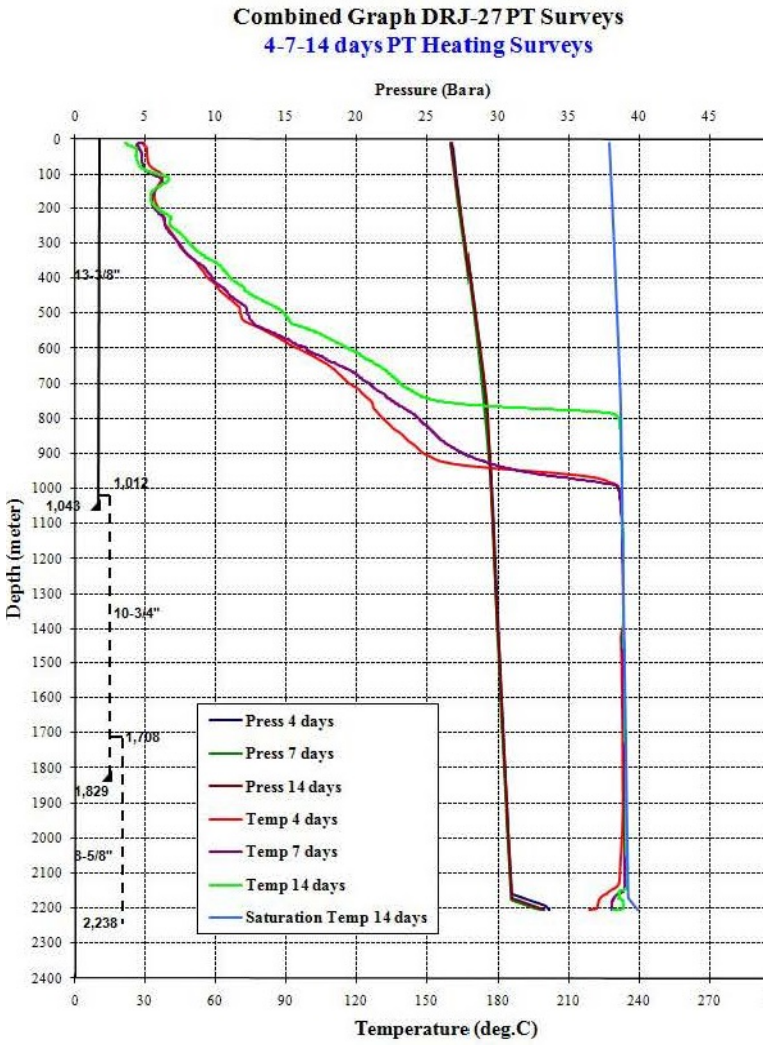

FIGURE 3: PT profiles in DRJ-27 (Hadi et al. 2010)

All the water properties are those for the pressure and temperature at that depth. The vertical pressure gradient exceeds hydrostatic by an amount needed to drive the natural flow upwards to surface. If the well contains a column which is in thermal equilibrium with the reservoir, the pressure gradient in the wellbore is hydrostatic for the reservoir temperature and it cannot be in equilibrium with the reservoir pressure over the entire open interval. If the wellbore pressure balances reservoir pressure near the centre of the open interval, it will be less than reservoir pressure in the lower part of the well, and greater than reservoir pressure in the upper part. If there are two or more permeable zones, fluid will flow into the well at the lower zone(s), up the well and exit at the upper zone(s). The fluid in the wellbore is no longer static and will not be in thermal equilibrium with the surrounding reservoir. Instead there will be a thermal equilibrium between heat conducted into or out of the well, and heat carried by the flow in the well. The details of this example are particular to a well drilled into the upflow part of the reservoir. In the particular case of Mak-Ban, the wells typically contain two-phase upflows, as illustrated in Figure 5 below. In other parts of the reservoir wells, may typically exhibit downflows. In an exploited field, the fluid distribution is highly disturbed and this can affect temperature-pressure profiles measured in the wellbore in various ways.

Rather than being a passive monitor of the reservoir pressure and temperature, the well must be considered as a pipe penetrating the reservoir, with connections to the reservoir at various depths. Fluid flows along the wellbore between these points (later referred to as "feed zones") depending on the permeability of the various feed zones and the pressure imbalance between the wellbore and the

reservoir at the different zones. . For the above reasons it is important when designing a well for monitoring reservoir conditions that the open hole length is small and ideally there is a single feed zone.

The well test examples used here are obtained from geothermal wells in different fields in several different countries. The wells and data have been selected as they make good examples of the various interpretation methods that can be used. In practice the data interpretation is usually more difficult than in the examples, due to missing information, unstable well conditions, transient changes in pressure and temperature, noisy data, or an incomplete well measurement programme.

Each well is an individual, and deserves special attention to get the best information about the underground resource. Sometimes, there is only one opportunity to obtain certain information during a well's lifetime, and if the appropriate measurements are not made in that period, then the opportunity has passed and cannot be later recovered.

- Injection capacity - flow/pressure characteristics

2. WELL MODELS

The object of measurement interpretation is to deduce from measurements made within the dynamic fluid inside the wellbore, the properties of the reservoir around the well.

Ideally, a complete interpretation provides a complete model of the well, including:

- Location and thickness of permeable zones
- Permeability of these zones, expressed as injectivity, productivity and/or transmissivity
- Reservoir pressure at each zone
- Reservoir temperature over the entire well depth
- Reservoir temperature or enthalpy of fluid at each permeable zone
- Any mechanical variation of the well – wellbore diameter, suspect casing, blockage, deposition

Usually only part of this information can be determined. Note that reservoir temperature may be found over the whole interval, as conductive heat flow into the well may control well temperatures, but reservoir pressure can only be determined at permeable zones, as it is only at these depths that the well communicates with the reservoir fluid pressure. Figure 4 shows a simple well model of a well under injection.

The following Figure 4 and Table 1 show an example of a well model being used to match discharging spinner measurements. Seven feed zones, including one thief zone and one cold zone, are needed. Downhole enthalpy, shown in Figure 5, is the enthalpy of the flowing mixture as computed from the pressure gradient and flow rate, using the drift-flux model for two-phase flow (Hasan & Kabir 2002), and allowing for frictional pressure drop.

Acuña (2003) reports that using such a well model provides better forecasts of future steam flow than decline analyses. A detailed well model helps to diagnose problems such as a cold intrusion at one feedzone, and plan repairs.

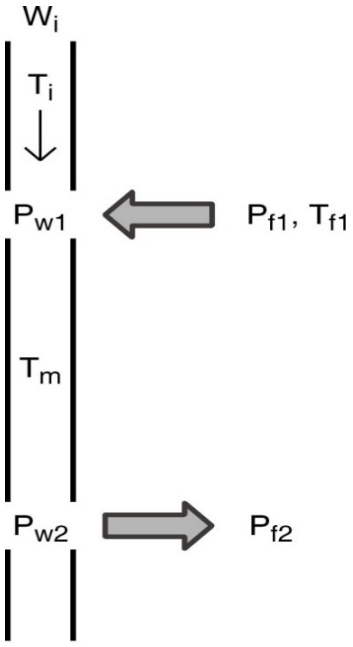

FIGURE 4: Simple well model – two zones

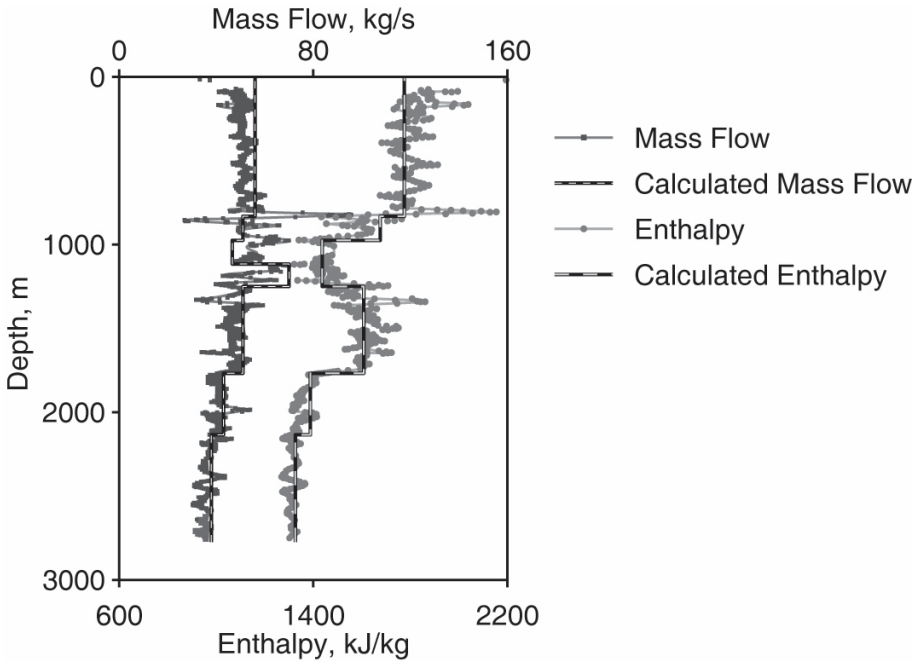

FIGURE 5: Calibrated well model

TABLE 1: Well feed zones
(Acuña & Acerda 2005)

Depth, m	Flow, kg/s	Enthalpy, kJ/kg
831	5	2791
975	9	2791
1116	-28	N/A
1250	19	977
1768	8	2791
2134	5	1861
2775	38	1326

3. SOME BASIC WELL PROFILES

3.1 Conductive vs. convective

The simplest distinction made in temperature profiles is between conductive and convective profiles. When rock is impermeable, heat is transported by conduction. This produces a characteristic profile where temperature increases linearly with depth – the gradient will change if there is a change in thermal conductivity of the rock.

Convection by contrast is a far more efficient means of heat transport than conduction. Once there is some permeability in the rock – and the required permeability is much less than what is needed for economic well performance – the fluid motion controls the temperature distribution. Convective profiles can take a considerable variety of forms, with isothermal sections, inversions, boiling sections and mixtures of these. Figure 6 shows temperature profiles from two wells at the EGS project at Soultz, France (Genter et al., 2009). There are three sections on the profile. The first kilometre has a high gradient and linear profile, indicating conductive transport. Then from 1 to 3.3 km there is a much lower gradient, which is attributed to a convective system along faults and fissure zones. Finally below 3.3 km there is again a

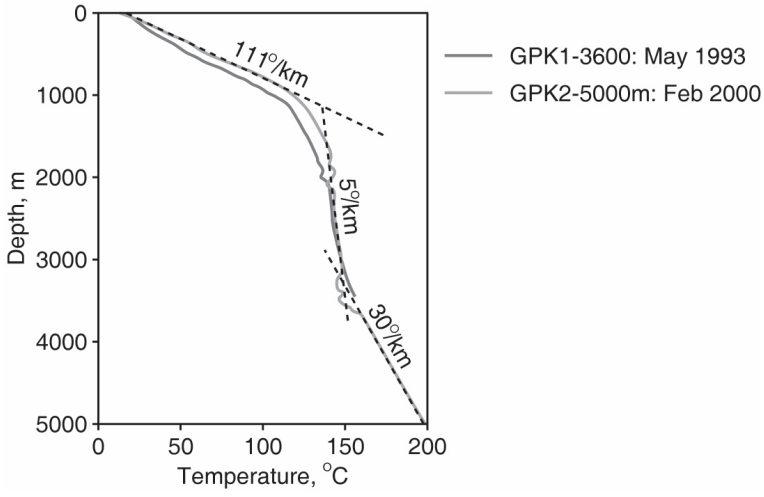

FIGURE 6: Temperature profile in Soultz

high linear gradient indicating conductive heat transport and consequently lower permeability in the surrounding formations.

3.2 Isothermal

An isothermal profile is a section of the well where the temperature is constant or nearly constant with depth. This can reflect circulation of fluid in a section of the wellbore, or interzonal flow (without boiling), or it may be that the reservoir itself has isothermal temperatures due to convection. Figure 7 shows three profiles in well NG13 at Ngawha. During injection there are inflows to the well at 960 m. At the inflow depth the temperature increases rapidly over a short interval, as the cold water being injected into the well mixes with the hot inflow. The mixture flows down the well and exits at a lower feed zone at 1600 m. In the shut-in condition the temperature profile looks similar to Figure 2, but in this case the isothermal section between 960 and 1600 m is due to interzonal flow in the wellbore. Below 1600 m the wellbore temperatures are again conductive. The pressure profiles show that during injection the pressure at 960 m is less than the stable shut pressure, and more than stable shut pressure at 1600 m, confirming that during injection there is inflow at the upper zone and outflow at the lower zone (without the need for spinner information). The stable shut pressure is in fact not reservoir pressure, as even when shut there is still a downflow between the two zones.

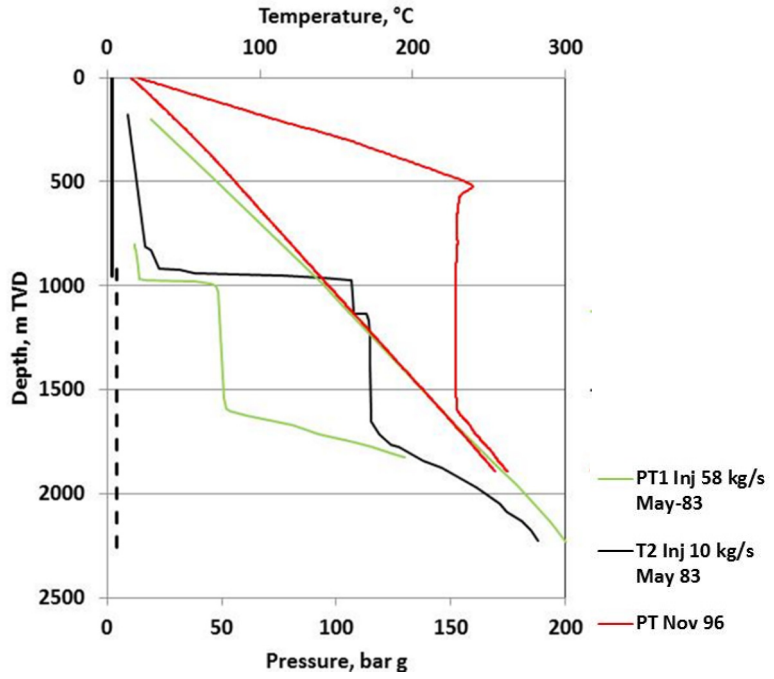

FIGURE 7: Temperatures in NG13

The water flowing down the well gains or loses some heat by conduction to the surrounding formation, but this amount is generally negligible unless the flow is small, in the order of one litre per second or less. There is also a slight heating due to the adiabatic (isentropic) compression of the fluid with greater depth and pressure.

3.3 Boiling curve

A boiling point temperature profile is a column of water which is at boiling point for the pressure, allowing for the effect of dissolved gas. Figure 8 shows two such profiles from well WK24 at Wairakei. These boiling point profiles are produced by an upflow in the well. In the 1955 profile, boiling water enters the well near 580 m and flows up, continuing to boil as it ascends. Boiling water exits the well at a shallow feed point between 350 and 400 m and the steam, together with non-condensable gas rises into the casing. In the 1958 WK24 profile, liquid water enters the well near well bottom and flows upward, boiling at 450 m. The boiling profile in both 1956 and 1958 obscures the detail of the shallow reservoir temperatures, which were inferred from heating measurements in WK24 and measurements in adjacent wells.

3.4 Two-phase column

A more extreme upflow is shown in Figure 9. Here two-phase fluid enters the well at a deeper feedzone and flows up the well, producing a column of two-phase fluid throughout the complete wellbore. Water and possibly steam exits at a shallow feed, some steam continues up the wellbore to condense in the casing if shut, or to bleed. In this case both reservoir temperatures and pressures are completely obscured.

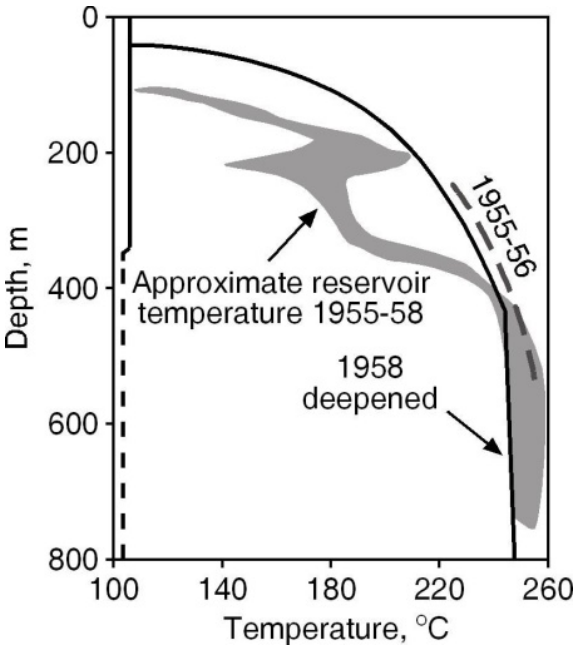

FIGURE 8: Temperatures in WK24

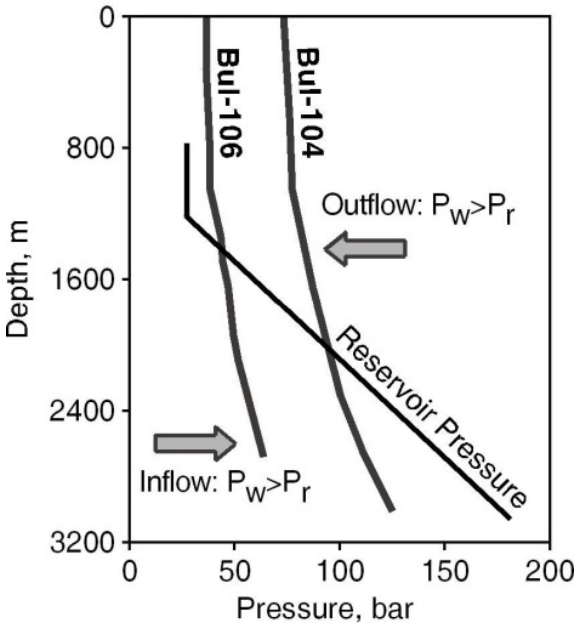

FIGURE 9: Pressures in Bulalo (Mak-Ban) wells (Menzies et al. 2007)

It should be noted that this profile in a well does not show a "two-phase gradient" in the reservoir – although these profiles do normally appear only in reservoirs with excess discharge enthalpy. There can be a genuine two-phase gradient in the reservoir, but that normally produces a very different downhole profile – a "steam cap", as shown in Figure 10. Such a downhole profile is of course also produced in a reservoir with a genuine steam cap. It is also produced in a reservoir that has only a steam zone with no water layer at all, as shown in Figure 11.

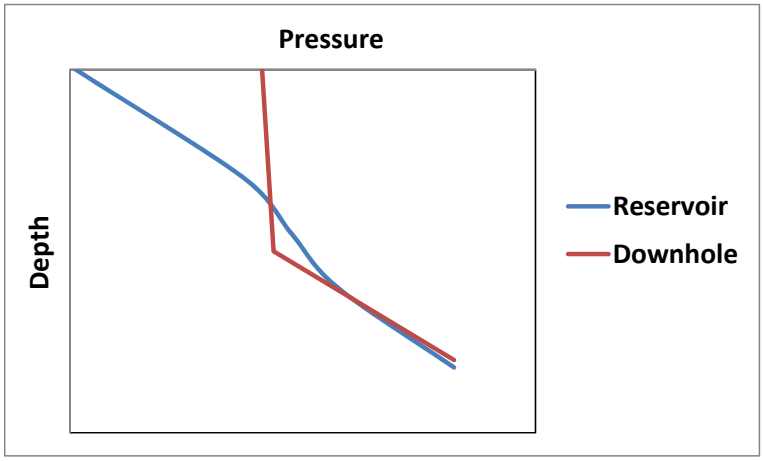

FIGURE 10: Two-phase reservoir profile and steam cap well profile

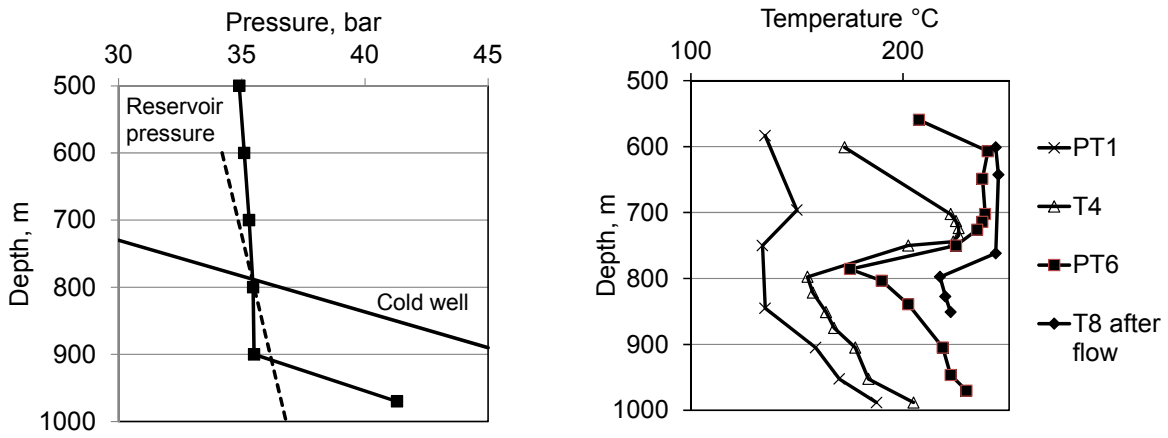

FIGURE 1: Pressure-temperature profiles in a vapour-dominated reservoir

3.5 Gas pressure at wellhead

When there is internal upflow in a well, and water boils, there is a flow of steam (and non-condensable gas) into the upper part of the well, and into the casing, depressing the steam-water interface with the result that a pressure is developed at the wellhead. When the shallow, cased-off formations are cold, heat is lost to the cold formations and with time the steam condenses and the remaining gas accumulates in the upper part of the casing. This process is the source of gas pressure build-up, which is frequently observed in high temperature boiling reservoirs, and can also occur in a reservoir with quite low gas content.

LECTURE 2

SPINNER MEASUREMENTS

1. INTRODUCTION

A spinner tool provides a profile of spinner frequency against depth. It depends upon the fluid velocity in the well, tool velocity and wellbore diameter. Simple interpretations are made by inspection of the frequency profile. To obtain a reliable fluid velocity profile requires up and down passes at two or more different tool velocities. To separate the effects of wellbore diameter requires fluid velocity at two or more different fluid flow rates.

2. CROSSPLOTTING AND TOOL CALIBRATION

A spinner is an impeller which is used to measure fluid velocity. The fluid flow causes the impeller to turn, with the frequency being proportional to the relative velocity between the tool and fluid:

$$f = (V_t - V_f)/C \quad (1)$$

or

$$V_f = V_t - Cf \quad (2)$$

where Vf is the fluid velocity, Vt the tool velocity and C is the pitch of the impeller in meters per cycle. It is assumed that the spinner measures a representative fluid velocity. If the wellbore is deviated the tool must be centralized as otherwise it will lie on the bottom side and may not measure a representative value. Figure 12a shows a typical set of good quality spinner measurements. Here there are two sets of down and up logs at 0.8 (black) and 1.2 m/s (red). Note that the profiles have the same shape, displaced by a (roughly) constant amount. This displacement, from Equation (1), is simply the difference in tool velocity divided by the calibration constant. In this case it is immediately apparent that there is a major loss zone at 1840-1865 m, where the frequency changes significantly, while there is no significant consistent change above 1840 m.

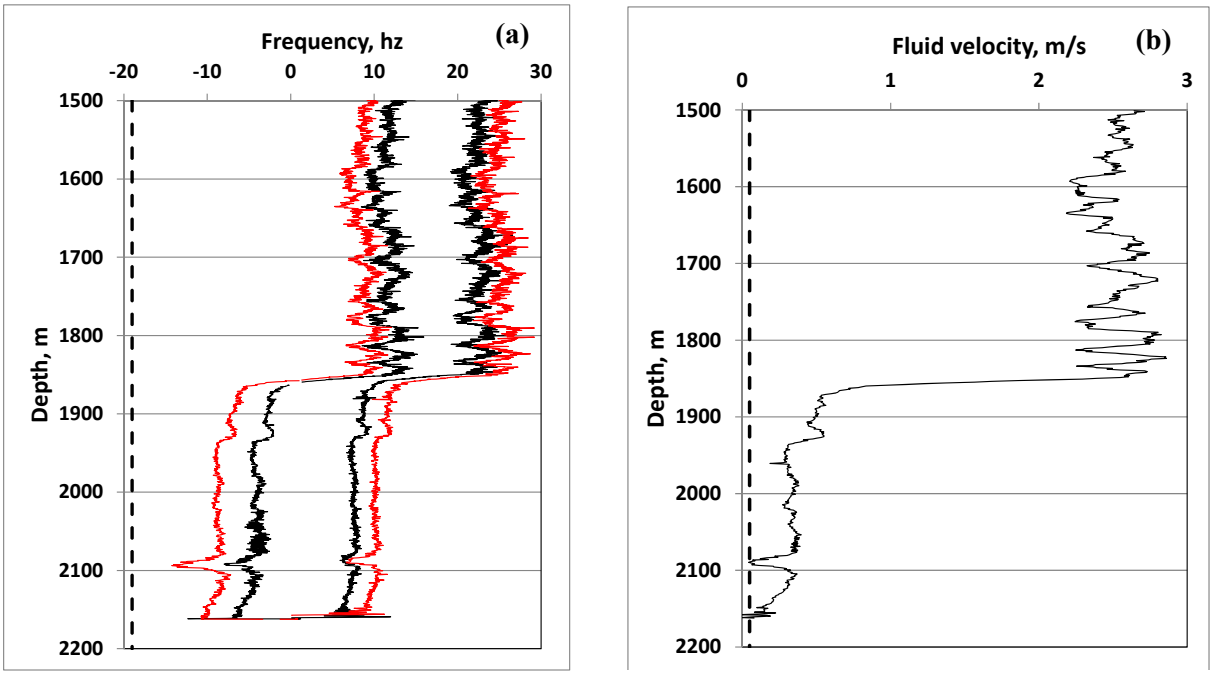

FIGURE 12: (a) Spinner data and (b) interpreted velocity

For analysis, spinner data is grouped into *stations*, or short intervals. Figure 13 shows *crossplots* of data in two stations, data within one station which in this case is a 1-metre interval. Figure 13a shows a linear relation between frequency and tool velocity. The line extrapolates to zero spin at a velocity of 2.6 m/s – this is the interpreted fluid velocity (as in ideal conditions the spinner would not rotate if the logging tool is moving at the same velocity as the fluid in the wellbore). For many geothermal wells a simple spreadsheet method can be used to obtain the fluid velocity – at least as a preliminary estimate using the following procedure:

- Check spinner frequency data for null values (and delete these - impeller may be stuck due to wellbore debris)
- Sort data by depth (over the interval where there are at least one up & one down profile)
- Check some crossplots of frequency versus log speed at several depths to see how many data points are required to obtain a reliable crossplot
- Using one of the built-in spreadsheet functions extrapolate a regression over a fixed number of data points to obtain the fluid velocity at the zero frequency intercept using log speed (y values) and spinner frequency (x values)
- Plot depth versus interpreted fluid velocity

This approach may provide a reasonable flow profile for many geothermal spinner logs. Accuracy of the calibration can be checked by comparing computed velocity within the casing against the expected velocity from the measured well flow rate.

Figure 13b shows data collected at another station where there is both positive and negative frequency data. There is a different linear relation for positive and negative frequency. That is, the effective pitch of the spinner is different depending on whether the flow is incident on the tool from above or below (As the impeller is usually located at the bottom of the PTS instrument flow from above and below the impeller is not symmetrical). This "bilinear' behavior is presumably due to detail of the impeller itself, and flow round the tool body, and is quite common. Equation (1) is then modified:

$$V_f = V_t - Cf \qquad f > 0 \tag{3}$$

$$V_f = V_t - Df \qquad f < 0 \tag{4}$$

Note that fitting a single line to the data in Figure 13b would result in an estimated fluid velocity that is erroneously low. In particular, it would also impute a non-zero velocity when the actual velocity is zero. Typically the constants *C,D* differ by 10-20% in good quality tool data but much greater differences occur quite often.

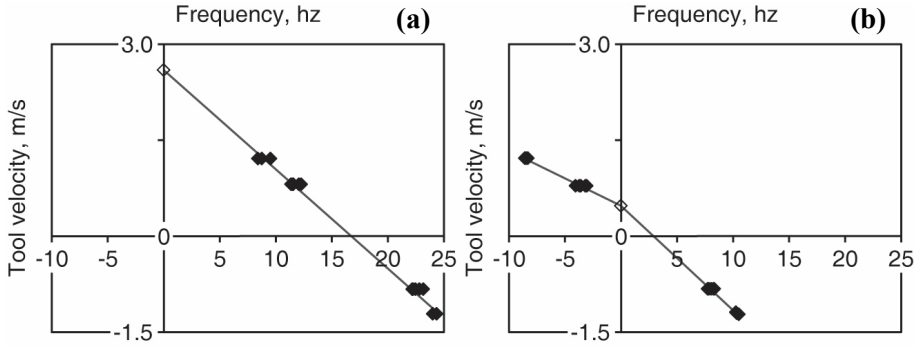

FIGURE 13: Spinner data crossplots. (a) Linear plot, (b) Bilinear plot

A best estimate of the fluid velocity can be found by regression. The data are grouped into stations. Let *i* denote the i^{th} station, and *j* the j^{th} data point within it. Equations (3) and (4) are written as:

$$V_{fi} = V_{tij} - Cf_{ij} + \varepsilon_{ij} \quad f > 0$$
$$V_{fi} = V_{tij} - Df_{ij} + \varepsilon_{ij} \quad f < 0$$

where ε_{ij} is the error. A regression is then performed, minimizing the total error, to find the velocity values V_{fi} and the calibration constants *C, D.* Spinner data is usually quite noisy. The fitted velocity is smoothed by the grouping of data into stations, and station size can be increased to reduce the noise, at the expense of lowered resolution. To make a bilinear spinner analysis requires data at two or more different positive and negative tool velocities. If there is only one pass up and down, or if all the frequency data has the same sign, a linear model must be used.

Data with zero or near zero frequency may lie off trend, due to spinner friction. The crossplot can look like Figure 14. Zero frequency data are often suspect, and it is best to avoid using many such data points.

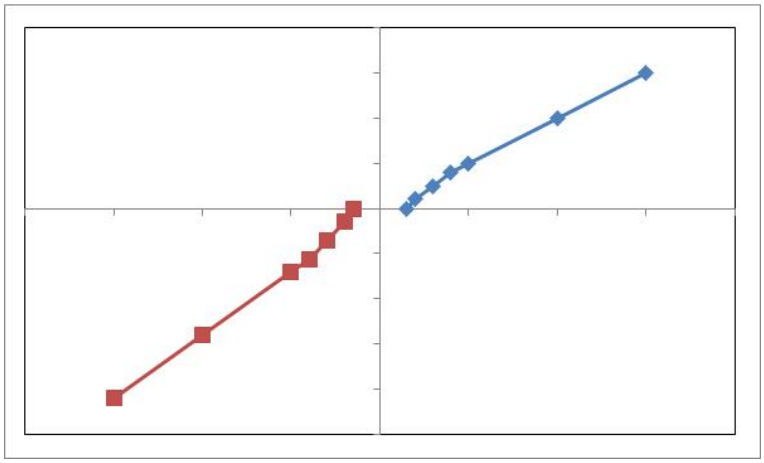

FIGURE 14: Crossplot – data near zero frequency off trend

If a regression is not done the next best alternative is to calibrate the tool by doing passes up and down in the casing (when setting the spinner logging program continue each profile into the cemented casing about 50 meters above the top of the perforated liner), crossplot the data to determine the effective pitch of the spinner, and then use Equation (1) to convert the frequency to fluid velocity – this also provides a cross-check that flow remains the same between the different spinner passes. As a last alternative the theoretical impeller pitch can be used, but this is not desirable as the actual pitch often differs significantly from this value especially at low frequency values, due to friction.

In a well with high fluid velocity, say a discharging steam well, fluid velocity is much larger than the tool velocity and it is not possible to calibrate the tool by fitting the data. A known tool calibration must be used, or simply the frequency data plotted as the effect of tool velocity will be small.

The spinner data collected at different tool velocity should produce profiles with frequency displaced by a constant amount, this amount being the pitch times the difference in velocity. The profiles in Figure 12a do show this. On careful inspection it can be seen that the profiles below 1860 m have a different displacement between the two positive frequency and the two negative frequency profiles compared to those above 1860 m. This reflects the different positive and negative calibration. If there is a feature on one profile that is not present on profiles at other velocities, and there was no change of tool velocity within the profile, this indicates a problem with the tool. Often, for example, the impeller can get blocked or slowed by debris.

3. INTERPRETING THE VELOCITY PROFILE

Figure 15 shows a result where the interpretation is straightforward, with the major loss zone clearly outlined at 920-940 m. Temperatures show inflows at the other two zones but these are not clearly shown by the spinner. However, in detail the spinner data can be somewhat more complicated, and more detailed and precise information can be extracted from the log with more detailed processing.

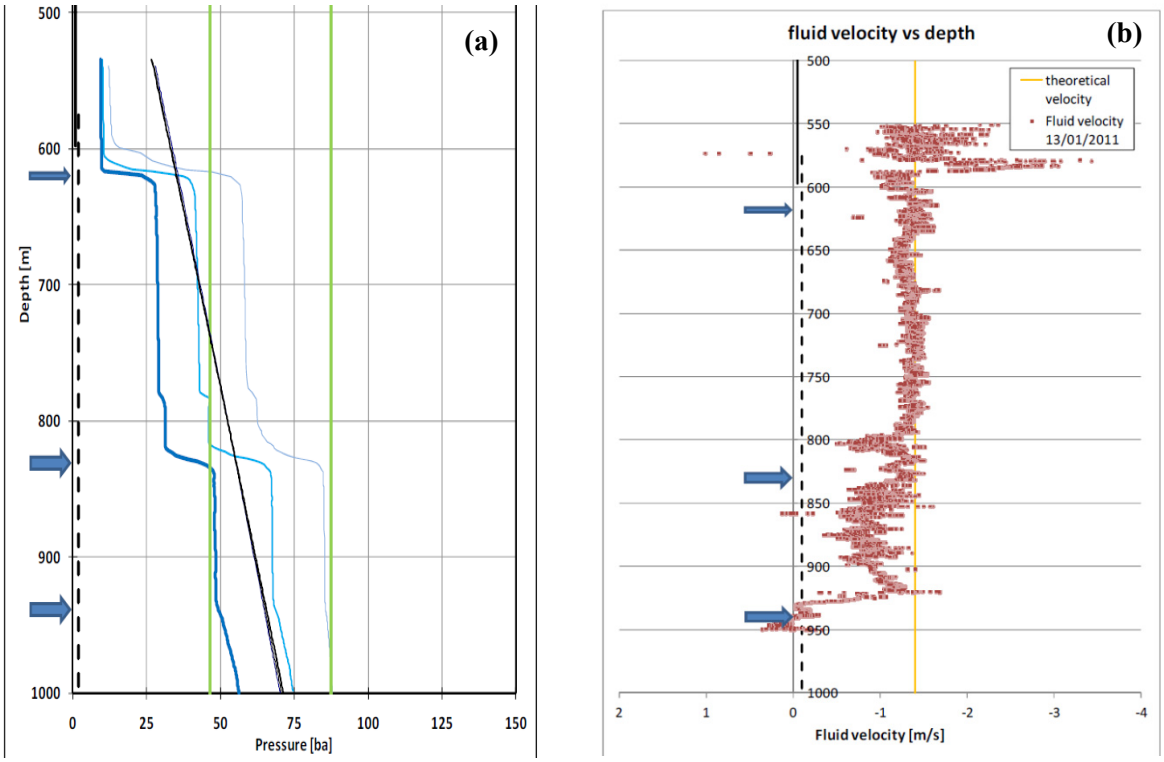

FIGURE 15: Spinner profile – successful result

4. WELLBORE RADIUS EFFECTS

Figure 12b shows the fitted fluid velocity profile from the data in Figure 12a. There is a clear loss zone from 1840-1870 m, where fluid velocity decreases from 2.5 to 0.5 m/s, so 80% of the flow is lost at this interval. The other loss zone is near the bottom of the hole, at 2100-2150 m. There is a lot of variation on the velocity profile. This is real, and is caused by changes in wellbore diameter. That it is real can be seen by comparing profiles at different flow rates – the variations due to wellbore diameter appear at all flow rates, whereas inflows and outflows change with the well flow rate. The dip in velocity just above 2100 m must indicate a significant enlargement near here. Above 1840 m there are irregular variations. There is often significant enlargement of the wellbore above the expected drilled diameter, due to erosion of the formation, particularly when drilling with aerated fluids. Often the wellbore is enlarged close to permeable zones, most likely due to increased fracturing of the rock in these areas. By comparing velocity profiles at different injection rates, it can be possible to separate the effects of wellbore enlargement and inflow/outflow (Grant et al. 2006)

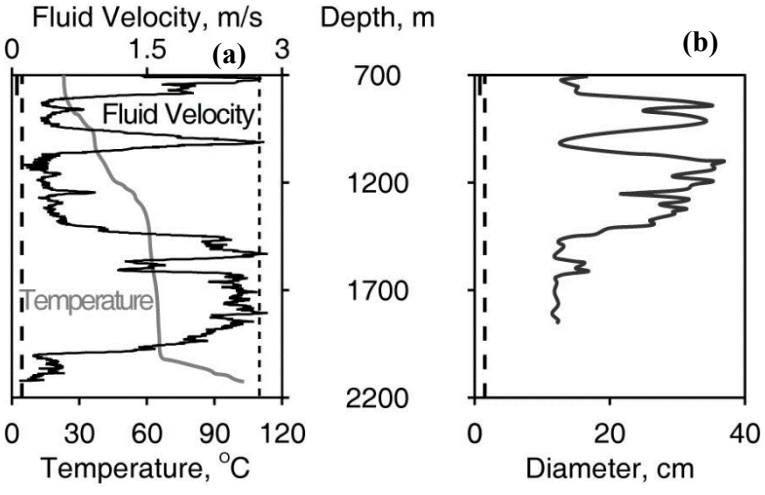

FIGURE 16: Spinner log in MK11; a) Fluid velocity, temperature and velocity inside liner; b) Wellbore diameter

Figure 16 shows an interpreted fluid velocity and temperature log for well MK11 while injecting 33 kg/s of cold water. The spinner frequency data from 4 up/down profiles was processed with 1 m stations. The well was drilled using an air-water

mixture for the circulation fluid to balance formation pressure. The temperature increase from 23 to 60°C indicates inflows broadly spread over the interval 800-1300 m, with no sharply-defined zone. Using the enthalpy balance method and assuming an inflow temperature of 250°C the inflow is relatively small at 6 l/s. In contrast to this relatively small inflow there are large variations in fluid velocity. There is a velocity peak at the casing shoe – there is usually turbulence at the liner top/casing shoe, which can make it quite difficult to detect a feed zone near the shoe. A similar maximum velocity at 1010 m, 1530 m and 1810 m suggests that the well is tight on the liner at these points, and there is much the same fluid flow at these points. The flow of 35 kg/s corresponds to a velocity of 2.8 m/s, shown as a dotted line in 15a. The maximum measured velocity is in good agreement with this. The large decreases in velocity 800-950 m and 1050-1430 m correspond to major enlargement of the wellbore. The well was drilled with aerated fluid, so significant enlargement can be expected. Below 1840 m velocity decreases steadily down to 2000 m. This corresponds to the major loss zone, and the temperature confirms that 2000 m is the bottom of the loss zone. The loss appears to be widely spread across the interval 1840-2000 m, with about half the loss concentrated within 1960-2000 m, but details could be confused by further wellbore diameter variations. Deviation in the well can cause some bias in spinner results, because the liner and the tool lie on the lower side of the wellbore and may not intercept a representative flow mixture. The magnitude of this bias is unknown but appears to be present in some cases.

Using the data down to 1840 m, it is possible to compute the wellbore radius, as down to this depth there appear to be no outflows. The total cumulative inflow can be calculated from a heat balance. Assuming an inflow temperature T_r = 250°C, based on measured temperature in the first heating run, and an injected flow of 33 kg/s which is at 23°C, the total flow at a depth above the first loss is given by a heat balance:

$$W(z) = 33 \times \frac{(H(T_r) - H(23))}{(H(T_r) - H(T(z))}$$

and the wellbore diameter *D* is given by

$$W(z) = \pi[D(z)/2]^2 \rho V$$

Figure 16b shows the computed diameter in cm. This calculation cannot be continued below 1840 m because velocity decreases due to fluid loss.

5. RATIO METHOD

When there are velocity profiles interpreted from sets of spinner profiles measured at two injection rates, comparison between them can separate the effects of fluid loss or gain, and variation in wellbore diameter. For each profile, the velocity profile *V(z)* is given by:

$$V(z) = W(z)/A(z)$$

where *W(z)* is the volume flow as a function of depth, and *A(z)* is the cross-sectional area of the well. The mass flow is expected to be piecewise constant function of depth, constant between feedzones and changing at each inflow or outflow. If we have two profiles at different flow rates, the cross-sectional area of the well is the same, and so the ratio of the two profiles should be constant, changing only at depths where there is fluid loss or gain:

$$V_1(z)/V_2(z) = W_1(z)/W_2(z)$$

6. DATA CORRECTION

Figure 17 shows profiles at two different injection rates. It can be seen that the details of the variation with depth are similar in the two wells. However closer inspection in Figure 18 shows some small differences.

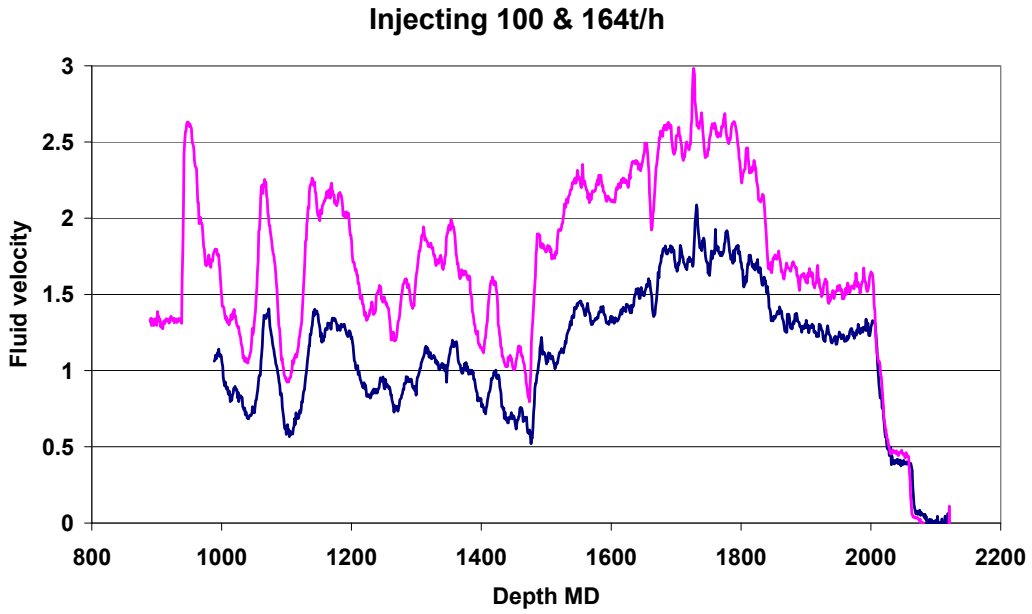

FIGURE 17: Spinner profiles at two flow rates (PK7 spin 100 tph plus comparisons.xls)

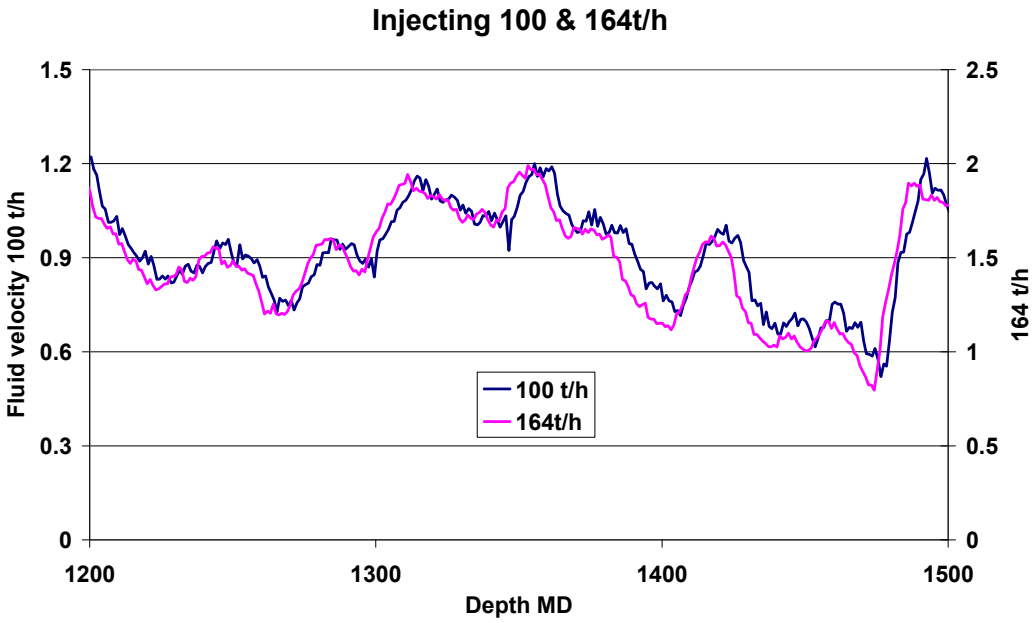

FIGURE 18: Detail of two profiles

This shows that one profile is slightly displaced in depth compared to the other, by 3.5 m. It is necessary to correct the depth to make the peaks and valleys coincide. The displacement is apparently due to tool calibration and/or cable stretch. This value was found by choosing the displacement that minimized the variance in the ratio in the interval 900-1500 m, where there are no loss zones. Figure 19 shows an example of the displacement in PT profiles.

Because the method compares between spinner profiles, it is dependent on good quality spinner data. Such data is now available, but typical data from older runs has proven to be too poor for the method to work.

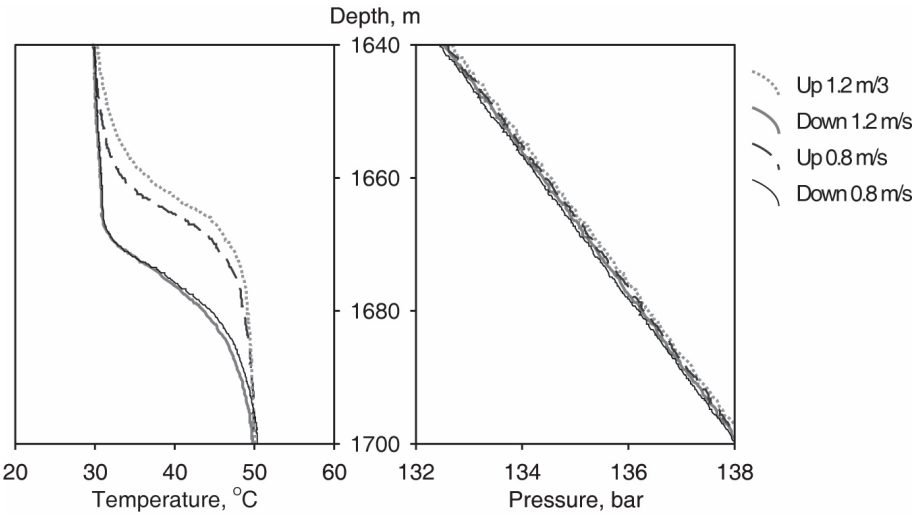

FIGURE 19: Displacement of PT profiles

7. RESULTS: INJECTION

Figure 20 below shows the ratio of the velocities at the two rates.

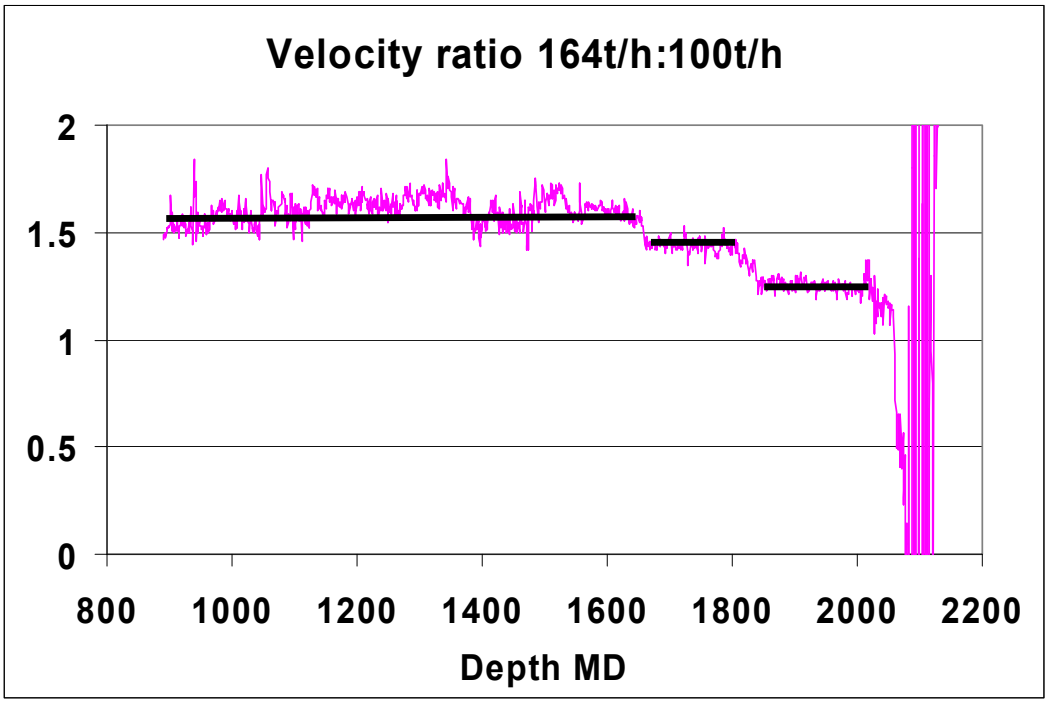

FIGURE 20: Ratio of velocities at two rates

Loss zones are identified at three depths:

- 1655-1675 m
- 1800-1855 m
- Below 2035 m

Note that the first loss zone is not identifiable in the individual spinner profiles. It is hidden by the noise created by variation in wellbore diameter, so that the relatively small velocity change due to fluid loss is not discriminated. As there is no loss down to 1655 m, the wellbore diameter can be computed from the known injection flow rate. This is shown in Figure 21.

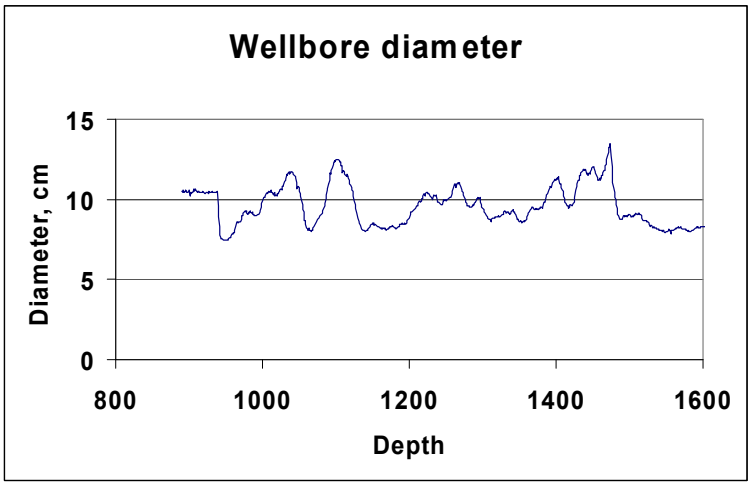

FIGURE 21: Wellbore diameter

8. HIGH FLUID VELOCITY

The discussion above relates primarily to measurements made with liquid in the wellbore. When the fluid velocity is large compared to the tool velocity, the change in frequency between up and down passes is relatively small, and cross-plotting is not effective as a means of calibrating the tool. Figure 22 shows a spinner run in a discharging steam well. Because the contrast between the two passes is small, the calibration must be taken from some other test, and applied to the frequency data to give fluid velocity. The pressure profile shows the steam-water interface below 1400 m, and the spinner indicates no significant flow below the first inflow at 1250 m, with a second inflow at 1100 m.

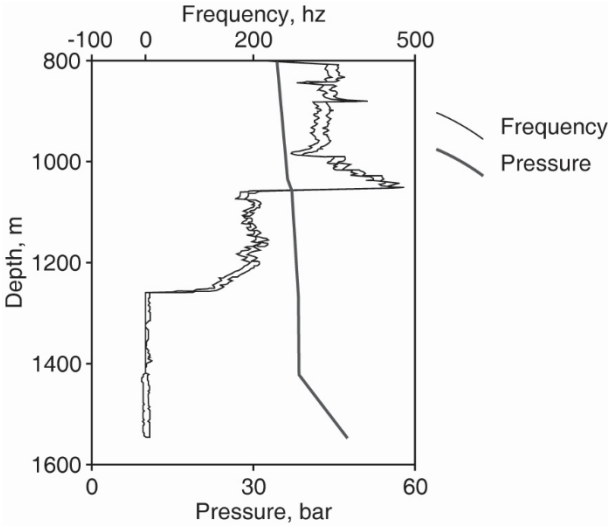

FIGURE 22: Spinner profile in dry steam well

9. DATA ERRORS

Spinner data often contains errors, and the results should be plotted as frequency against depth to check for these. Figure 23 shows one problem that sometimes occurs. The data is all of one sign. The spinner has failed to report negative spin in the down pass. Some spinners do not report sign and give only the magnitude of the spin. In this case it can be seen that a section of the data should have negative sign, and the corrected version is shown on the left. This can be recognized by the comparison against the up pass, and by the way the data 'bounces' off the zero frequency axis.

Figure 24 shows some other errors. In the left hand figure there are sections of anomalous data. For some reason the spinner produced spurious results during these segments. Possibly there was some debris stuck in the tool. The right hand figure shows outliers, spurious high values and spurious zero values. These should be removed before analysis. Zero frequency values are usually suspect as the propeller can stick at low frequencies.

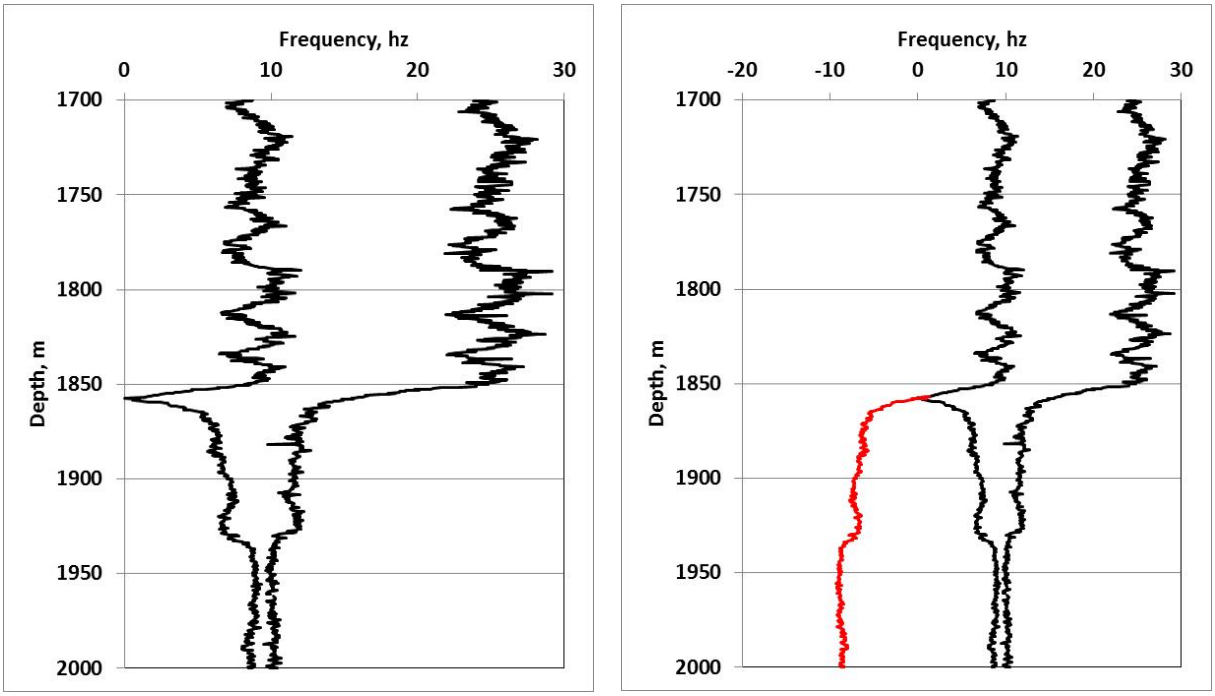

FIGURE 23: Data with sign error

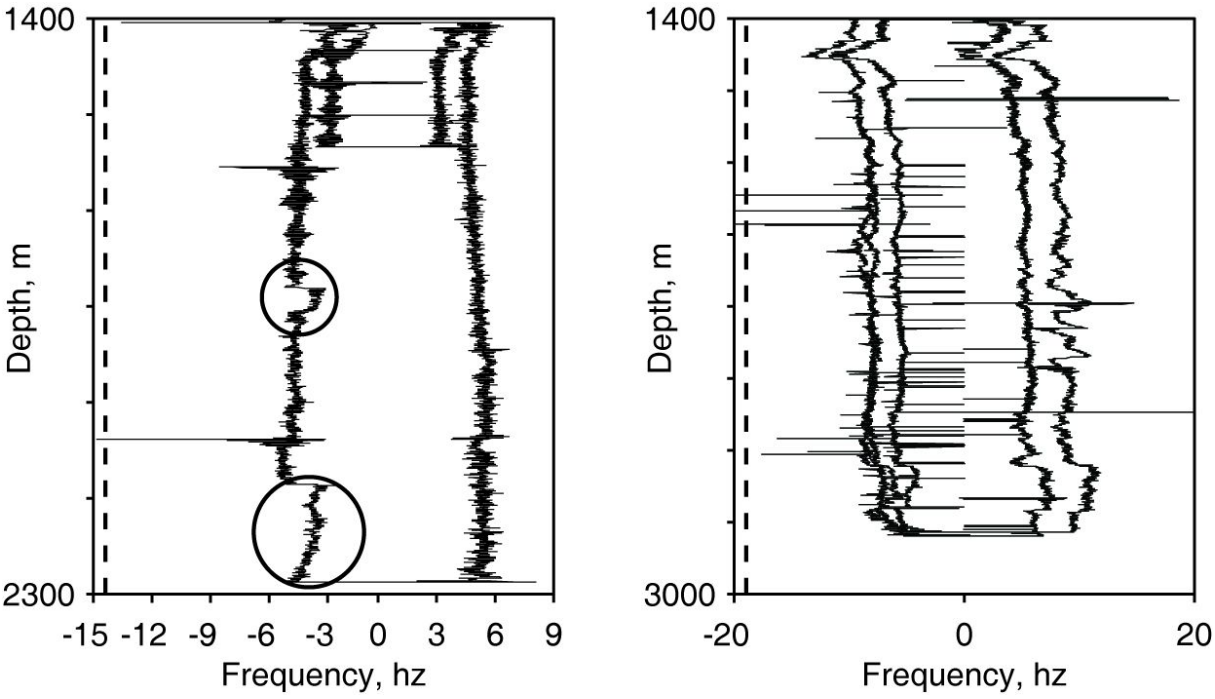

FIGURE 24: Errors

Finally, not an error but a common effect, is shown in Figure 25. There is a region of low velocity at the liner top.

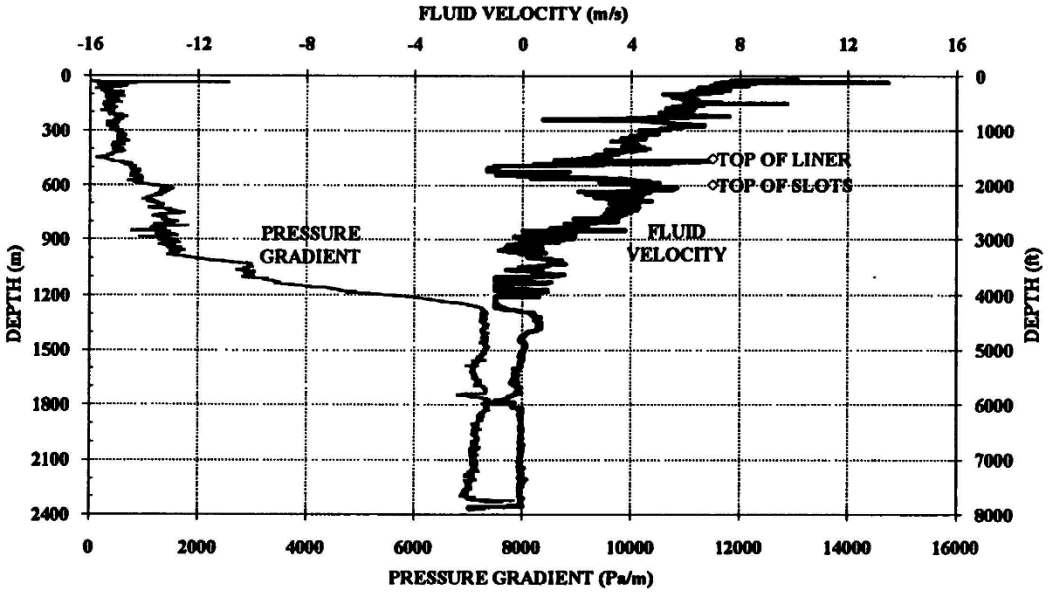

FIGURE 25: Effect of liner top

LECTURE 3

HOW PERMEABLE?

It is common to refer to wells, fields or structures are permeable or impermeable. This can be a careless oversimplification. Permeability is a ***number***. "Permeable" or "impermeable" are only valid in relation to some criterion.

1. WELL PERMEABILITY

For example, the following criteria (Figure 26) *approximately* describe permeability as used in relation to wells in New Zealand:

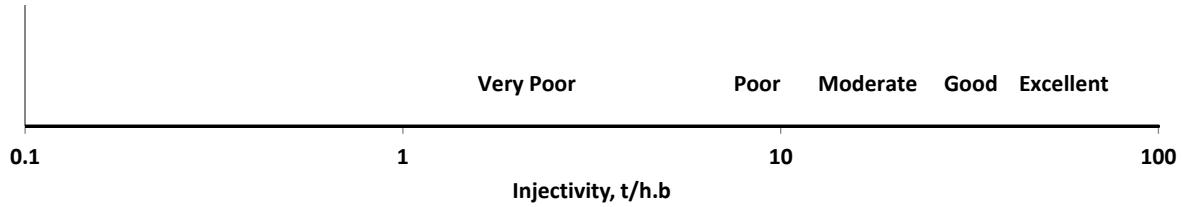

FIGURE 26: Well permeability scale

Poor permeability: injectivity < 10 t/h.b (3 kg.s.b)
Moderate permeability: injectivity ~ 20 t/h.b (6 kg/s.b)
Good permeability: injectivity ~40 t/h.b (9 kg/s.b)
Excellent permeability: injectivity > 50 t/h.b (15 kg/s.b)

That is very rough but at least it is a specific guide. Note that actual values extend over a very wide range, from < 1 t/h.b to values too large to measure, but at least several 100 t/h.b. Note also that acceptable permeability varies with temperature – with production from high (>300°C) temperature, wells operate with large drawdown and will give economic flow with lower permeability than if producing liquid at say 240°C. The injectivity gives a rough guide to the expected production, as shown in Figure 27.

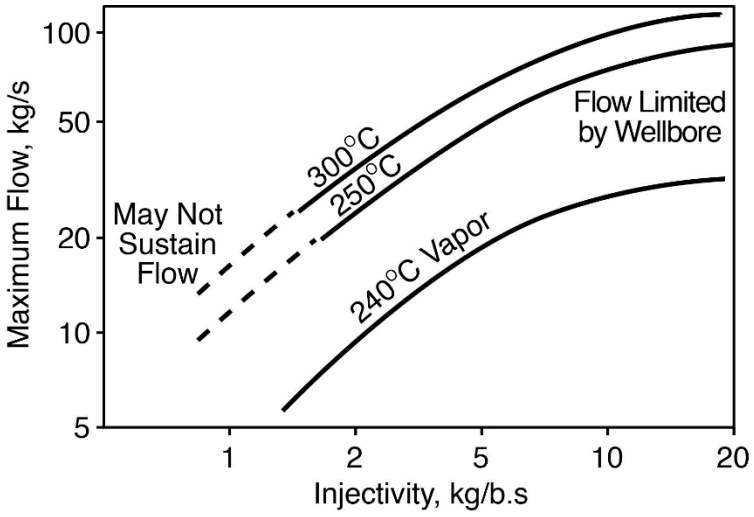

FIGURE 27: Expected production related to injectivity

2. DRILLING LOSSES

A sudden loss or gain of circulating fluid during drilling indicates that a connection between the wellbore and the formation permeability/fracture network has been established. The degree of permeability that is indicated depends on the balance between formation pressure and pressure in the wellbore at the permeable zone. Consider a well being drilled with water in a reservoir with hydrostatic pressure from ground surface. Measurements in other wells have established a reservoir pressure gradient:

$$P = 0.083 \times z + 1$$

where P is the pressure in bars, and z is the depth in metres.

Assume that while drilling at 1500 m depth using cold water (15°C) there is a loss of 19 l/s. Reservoir pressure at this depth is 0.083×1500+1=125.5 bar. The pressure due to a static column of water.in the wellbore is 0.098×1500+1=148 bar, so there is a pressure difference of 22.5 bar between the wellbore and the reservoir at the 1500m loss zone. The pressure difference is likely to be greater than 22.5 bar because of the increased density of the circulating fluid due to the drill cuttings being returned to the surface. The loss is 19 l/s, giving an injectivity of 0.9 l/s.b. Although the quantity of the loss is significant, because of the large pressure difference between the wellbore and the formation, it does not correspond with high permeability, and in this case the injectivity index value of 0.9 l/s per bar is unlikely to be sufficient to sustain an economic production flow.

If the reservoir is underpressured, even larger losses are possible with smaller injectivity. Estimates of injectivity, based on changes in circulation fluid returns during drilling only provide indicative injectivity values. The permeable zones are likely to be blocked by drilling fluids and cuttings and the injectivity may change with time as these materials are removed by washing of the hole or by discharge. The interpretation is different when drilling with fluids other than water. If mud is used as the circulating fluid the natural fracture permeability will almost certainly be impaired. If downhole pressure measurements are available while drilling, the combination of the downhole pressure record and drilling loss, against depth can be used to give the injectivity of the well as a function of depth. Ideally, a profile of the well can be determined, with injectivity of each loss zone measured, although in practice after the first major feed zone has been encountered the interpretation of subsequent changes in circulation returns are difficult to assign to particular depths.

3. FORMATION PERMEABILITY

It is more difficult when classifying formations or structures. Figure 28 shows tracer returns from tests at Wairakei. At first appearance this shows a very common observation. There are preferential returns along the faults, showing these to be the permeable paths. The isotherms too tend to follow the faults.

Closer examination shows a different story. The faults divide the reservoir into blocks. Tracer spreads relatively quickly within each block, but is delayed crossing into the next block. The faults are barriers, not permeable features, and the returns follow the faults because the barriers channel the flow.

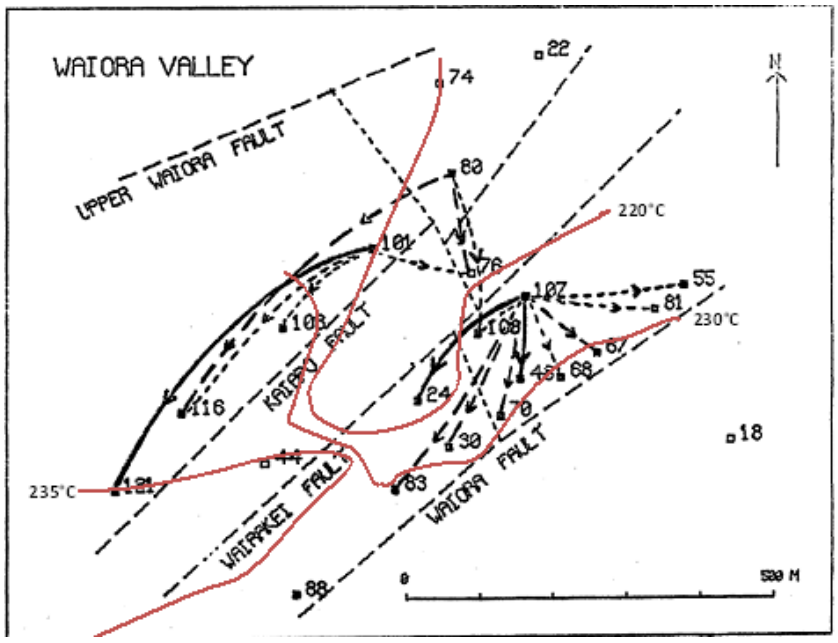

FIGURE 28: Wairakei tracer returns
(McCabe et al. 1980; Grant 1987)

More detailed information shows that the permeability structure is as shown in Figure 29 below. The largest permeability is horizontal, at formation contacts. These have kh's in the order of 100 dm, and are the structures providing productive permeability. The faults have kh's on the order of 1 dm, and are the primary vertical channels. Thus, for the purposes of horizontal flow the faults are "impermeable" (or more accurately, less permeable). For the purposes of vertical flow, the faults are permeable.

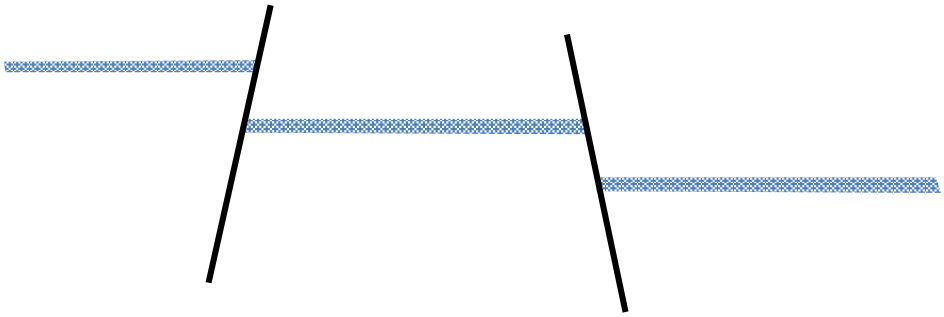

FIGURE 29: Idealised permeability structure at Wairakei

4. MONTE AMIATA

The Mt. Amiata system (Barelli et al. 2010) hosts a shallow reservoir and a deep reservoir. The temperature profile (Figure 30) shows that the two reservoirs are separated by a conductive zone between the two convective temperature zones. However there is, within the data scatter, a common pressure gradient implying a hydrologic connection (Figure 30). However these indications need not be contradictory. The temperature profile implies that vertical permeability in the conductive interval is less than some figure, $k_v < k_1$. The lack of an observable pressure difference implies that vertical permeability exceeds some other figure, $k_v < k_2$. It is possible that $k_2 > k_1$, so that both criteria can be satisfied. To be more precise would require modeling the system to determine how low the permeability must be to show the conductive gradient, and how high it must be to create the common pressure gradient. In the actual event, under exploitation no pressure interference has been observed between the two reservoirs.

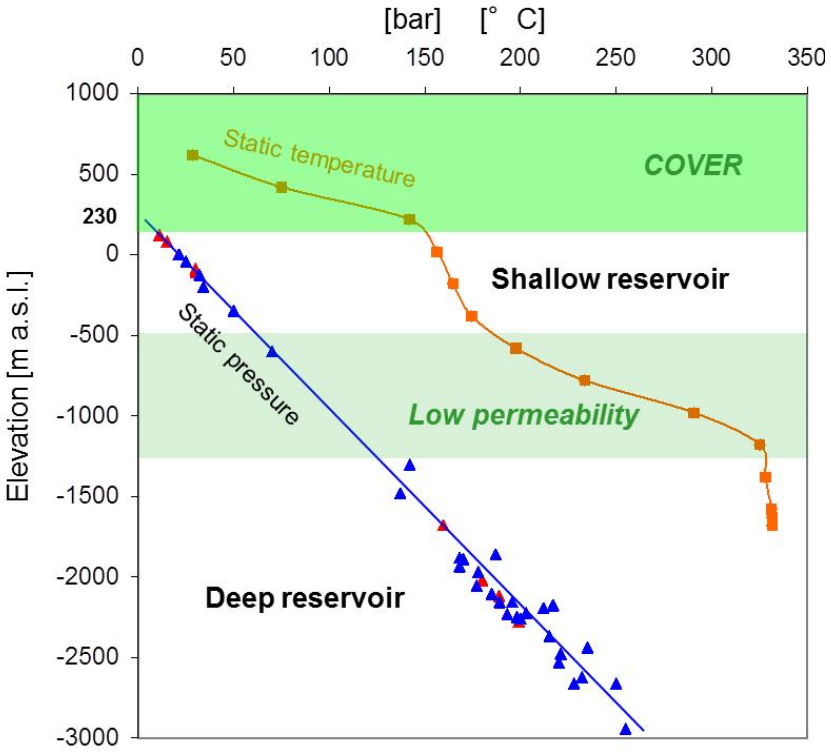

FIGURE 30: Mt Amaita PT profile (Barelli e al. 2010)

5. IMPERMEABLE UPFLOW

This is a fairly common observation. A field has an area of good productive permeability but extending drilling into the upflow finds high temperatures but poor permeability. How can this be? The reason again is sloppy use of "impermeable". To host the upflow of a geothermal field requires vertical kh's of the order of 1 dm. This can mean vertical permeabilities of a few md. This is not enough to support a good well. The upflow is "permeable" for the purposes of the natural flow in the field, but "impermeable" so far as production goes. The productive area of the field has higher permeabilities – that's why the outflow went there – and that supports productive wells. But in the end the incongruity is not the impermeable upflow. It is that there happens to be an area of higher permeability.

6. HOW TO MEASURE PERMEABILITY?

By application of Darcy's Law.

6.1 Vertical permeability - Ohaaki

Figure 31 sketches a cross-section through Ohaaki (Broadlands) geothermal field, concentrating on the shallow structure. The main reservoir extent is generally well outlined by the 250°C contour. The shallow formations are a number of rhyolites, split into Group 1 in the centre of the field and Group 2 to one side.

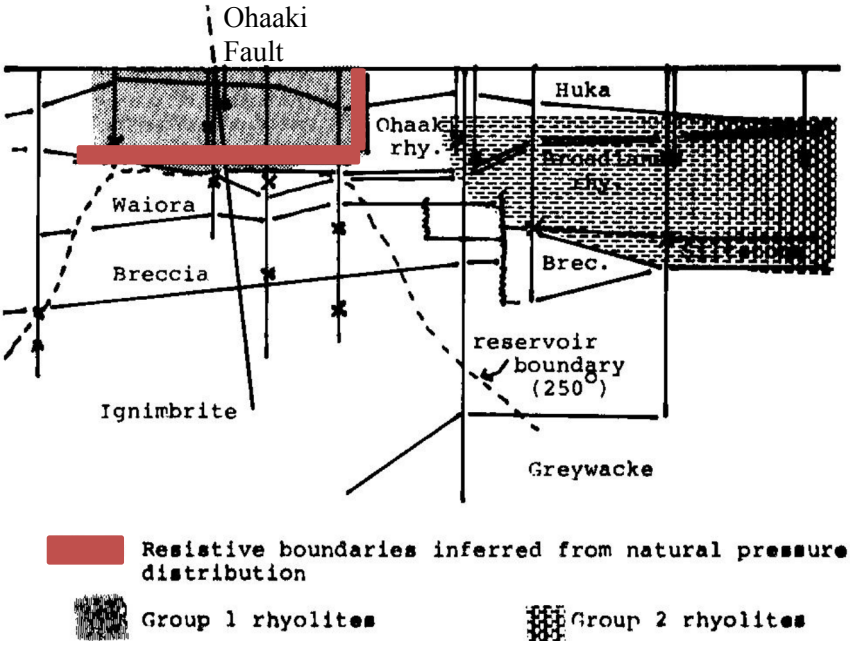

FIGURE 31: Ohaaki cross-section

The most prominent geological feature is the Ohaaki Fault, passing through the centre of the field. The largest surface feature, Ohaaki Pool, lies on the fault trace. Interference testing among shallow wells defines a clear division between the two rhyolite groups. Wells in each group mutually interfere but there is no communication between the groups. The responses in Group 1 showed a linear pressure drop with cumulative discharge and storativity of a free surface. This shows that the group is laterally isolated. Interference extends to groundwater wells, confirming the free surface. These wells are also known to communicate, poorly, with the deeper reservoir.

There is another boundary near the base of the Group 1 rhyolites. This is shown by the pressure distribution, shown in Figure 32. There is a displacement of about 6 bar between the pressure trends below the bottom of the rhyolite, and above.

The pressure differential of 6 bar (deviation from hydrostatic) can be used to measure the permeability of the Ohaaki Fault, which is presumed to be the channel providing the connection, albeit poor, between the deeper reservoir and the rhyolites above. The fault has a length of about 1 km across the field. There is about 100m distance between the base of the rhyolite and the permeable zones above. The natural flow is about 70 kg/s, nearly all of which discharges at Ohaaki Pool. Applying Darcy's law:

$$W = \frac{khL}{\nu}\frac{\Delta P}{\Delta z}$$

gives kh = 1.5 dm.

6.2 Vertical permeability - Kawerau

Figure 33 shows the initial pressure distribution with depth in Kawerau geothermal field. The pressures are feedpoint pressures in early wells, measured before much production had occurred. The wells are all located in one part of the field, and do not include southern areas drilled later. Within the data scatter, there is a single linear trend of pressure with depth, with a gradient of 0.085 bar/m. By comparison, the average reservoir temperature is 250°C which would have a hydrostatic is 0.078 bar/m. The difference between these values is 0.007 bar/m = 700 Pa/m which drives the upflow through the reservoir. The natural discharge from Kawerau has been estimated at 80MW. With a deep recharge temperature of 290°C, this represents a flow of 67 kg/s. If the area of upflow is A, and the vertical permeability k_v, applying Darcy's Law in the vertical direction gives

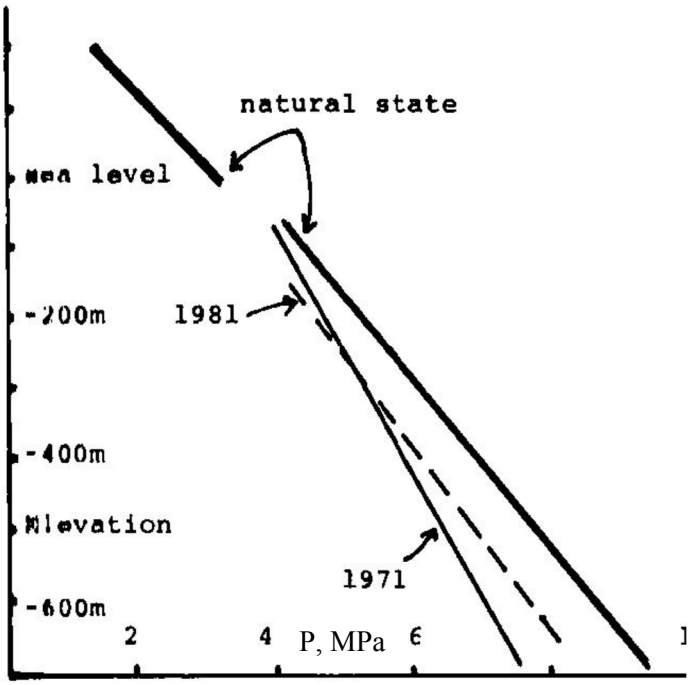

FIGURE 32: Pressure-depth trends in Ohaaki

$$W = 67 = \frac{k_v A}{\nu}\left(\frac{\partial P}{\partial z} - \rho_w g\right) = \frac{k_v A}{0.13\times10^{-6}}\,700$$

$$k_v A = 1.25 \text{ x } 10^{-8} \text{ m}^3 = 12.5 \text{ md.km}^2$$

If the upflow rises over an area of 1 km^2, the vertical permeability is 12.5 md. By contrast, interference testing among the wells shows *kh* values of the order of 100 dm or greater. On the gross scale, horizontal permeability is much better than vertical.

However the single measurement of an average vertical and horizontal permeability is not the end of the story. Figure 34 also shows a simulation match to the initial pressure. Note that there is a region of increased gradient at 500m depth. This resistance is also apparent in the interference tests. There are both deep production wells plus a number of shallow (<500m) wells – monitor wells and old shallow production wells that no longer produce. There is a clear separation between the two groups, with no interference between them. In contrast all the deep wells interfere, with high permeability (*kh*'s of hundreds of dm) extending over kilometres.

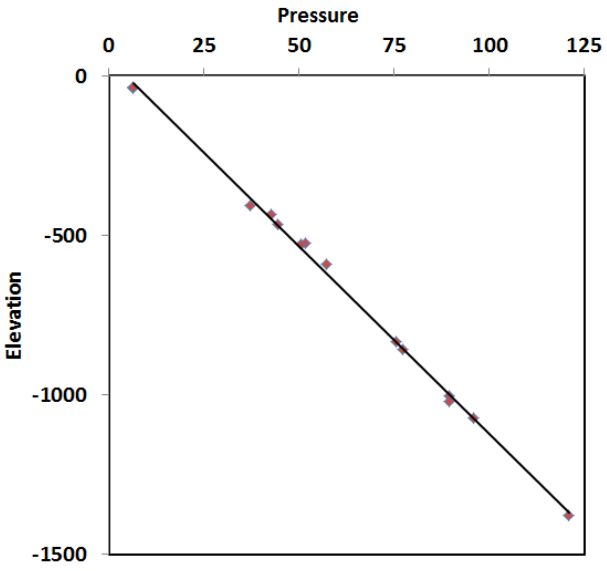

FIGURE 33: Pressure-depth distribution at Kawerau

6.3 Horizontal permeability – Kawerau

Figure 35 shows a map of Kawerau geothermal field. This is a high-temperature liquid-dominated field with high permeability. The red dots on the map are wells which have been shown to interfere with one or more of the other wells in the group. For many of the other wells there are no observations. There are no confirmed nulls (definite non-responses) within the area of known response from wells which reach production depths. There are nulls involving shallow wells above the reservoir.

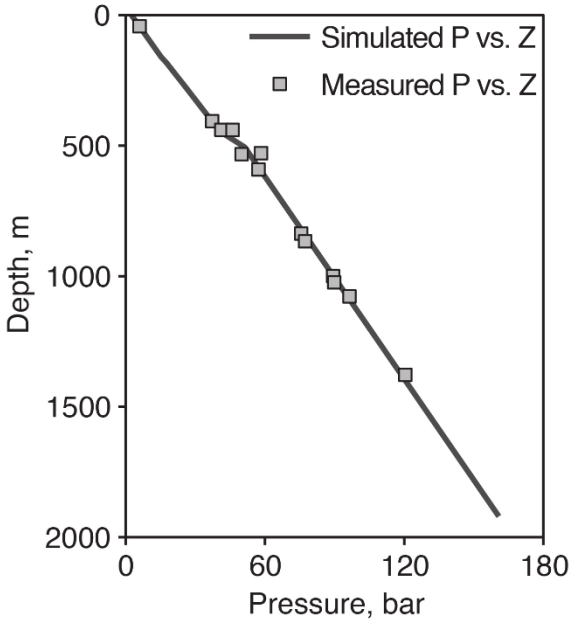

FIGURE 34: Pressure-depth distribution at Kawerau

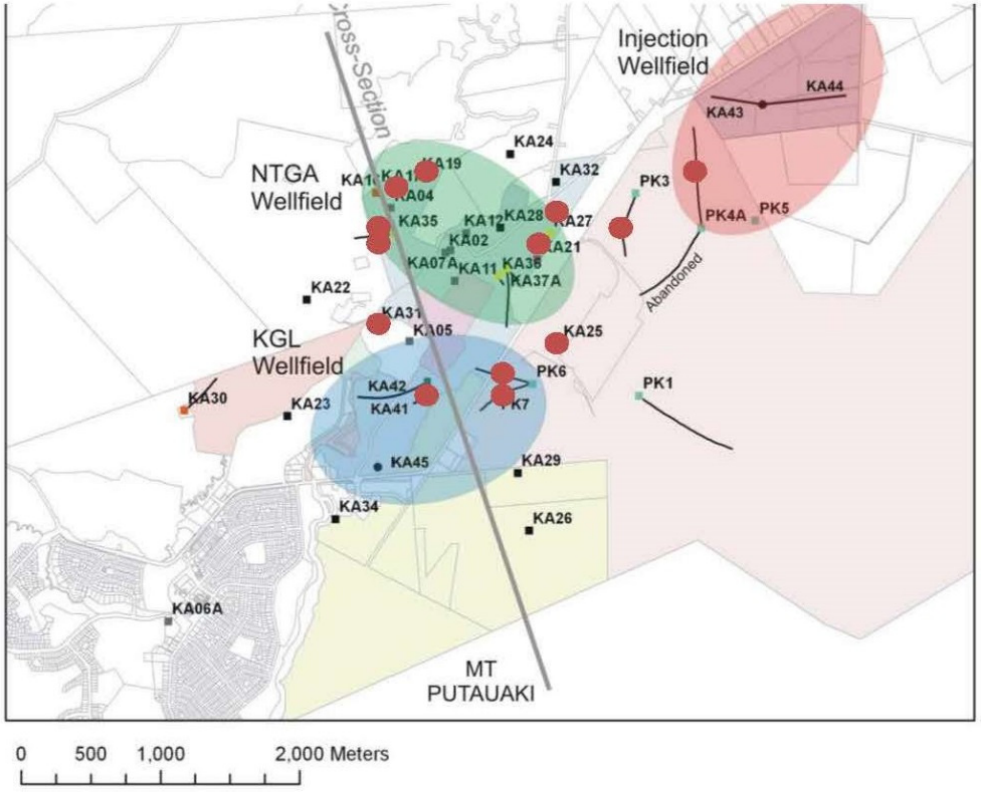

FIGURE 35: Wells observed to interfere at Kawerau (Grant & Wilson 2007)

The actual *kh* values vary significantly. Taking averages of log(*kh*), the average transmissivity is 160 dm, with a variance of a factor of 2. Permeability varies by orders of magnitude and arithmetic averaging is not appropriate to describe such a distribution. Often permeability follows a lognormal distribution and this is the case here, as shown in Figure 36.

One problem with interference testing is that it can be difficult to discriminate between a connection of high permeability and a partial connection. Figure 37 shows the problem. There is a reservoir with a main producing aquifer, with transmissivity *kh*. Above this aquifer is a resistive layer which allows some communication. Then there is a second smaller aquifer, and above that groundwater. Suppose that this upper layer has leaky connections to both the deep aquifer and the groundwater, and that the leak to groundwater is ten times larger than the leak to the deep aquifer. Pressures in the shallow aquifer can mirror those in the deep aquifer, but with only one-tenth the magnitude. The response of a well in the shallow aquifer will be about one-tenth that of a well in the deep aquifer. If it is analysed as a response in a single aquifer connecting the two wells, the imputed *kh* will be ten times the deep aquifer. (Because the magnitude of the response is one-tenth). So it can look like communication through an aquifer of very high permeability, but actually is communication through a leak into an aquifer of lower permeability.

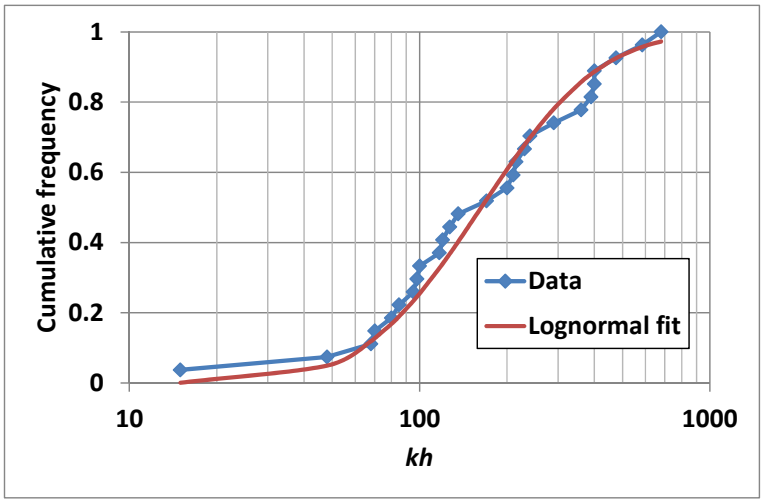

FIGURE 36: Distribution of interference *kh* values

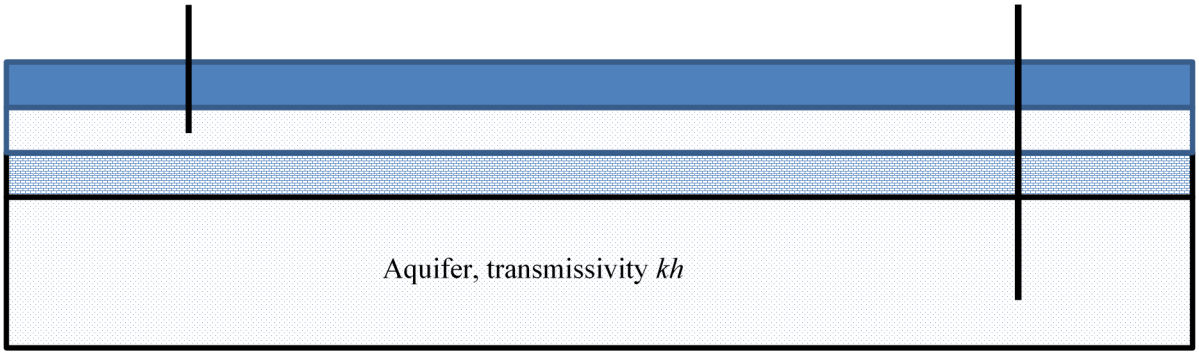

FIGURE 37: Aquifer with partially communicating aquifer above

All the different permeability structures are, in principle, tested by modelling. The model calibration uses the same data discussed here and in principle applies the same tests. However it is important to note that these calculations to determine permeability depend on relatively small pressure differences, sufficiently small that they are easily overlooked in the noise of a model match.

LECTURE 4

CONCEPTUAL MODELS OF GEOTHERMAL FIELDS

1. INTRODUCTION

A conceptual model is a concise qualitative description which contains the important physical elements and processes that determine the reservoir's behaviour, and is capable of matching the salient behaviour or characteristics of interest to the modeller. It is important to be explicit about the conceptual model – often there are implied assumptions about what is typical that are assumed without consideration.

For example, in the early days of geothermal, scientists who came to geothermal from a petroleum background often presumed that a reservoir looks like Figure 38 – a sealed box, defined by capping layers above and below:

FIGURE 38: Reservoir as sealed box

If the scientist came from groundwater, the reservoir would be open at the edges – i.e. an aquifer, stratigraphically defined.

If you consult older material from New Zealand, you will see the following (Figure 39) as a "typical" geothermal field:

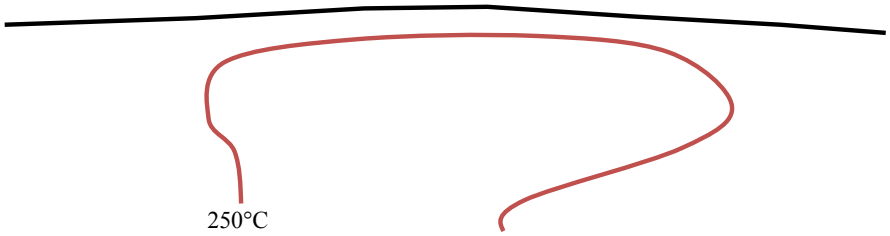

FIGURE 39: Typical New Zealand geothermal field

This is typical of New Zealand – relatively flat countryside and an upflow unrelated to other structure. Figure 43 shows a recent example.

Turning to Indonesia and The Philippines, one sees a picture like this (Figure 40):

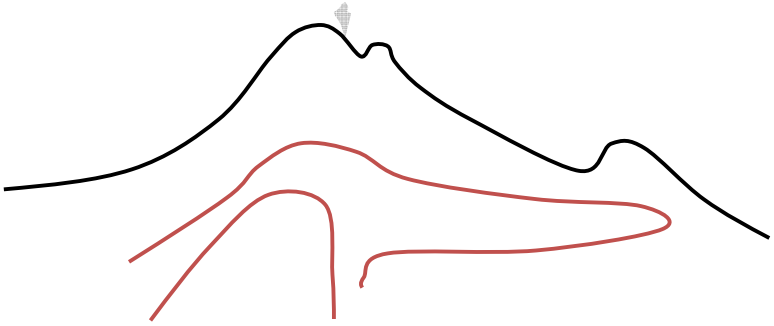

FIGURE 40: Typical volcano-hosted geothermal field

The geothermal field is directly associated with a volcanic centre, the upflow rises under the volcano, and has an outflow of water going downslope. Figure 41 shows a completely different picture: the crucial elements of the field are the fault structure, which determines the location of the upflow.

Each of these reflects what is typical in the area.

What the reservoir engineer brings to the conceptual model discussion is quantitative inference.

A conceptual model is a concise graphic and verbal description of the reservoir which combines the relevant structures and processes that determine its existence and response to exploitation. It is most commonly represented as a cross-section, or map, or both together. Figure 40 shows a very common example for a high-temperature system where there is significant topographic relief. The characteristic pattern of steam-heated features at higher altitude and chloride springs at lower altitude which identifies the point where liquid the upflow reaches the ground surface – at elevations lower than the steam discharges. The pattern of isotherms, alteration and surface activity is a consequence of the natural flow. As a contrast, Figure 42 shows the low-temperature system at Landau in Germany. This example says that the reservoir is defined as the aquifer, and the only significant information is the geology that defines its depth, and the increase of temperature with depth. This is essentially the groundwater version of Figure 38. Figure 43 shows a variant of Figure 39, and Figure 44 a variant of Figure 40.

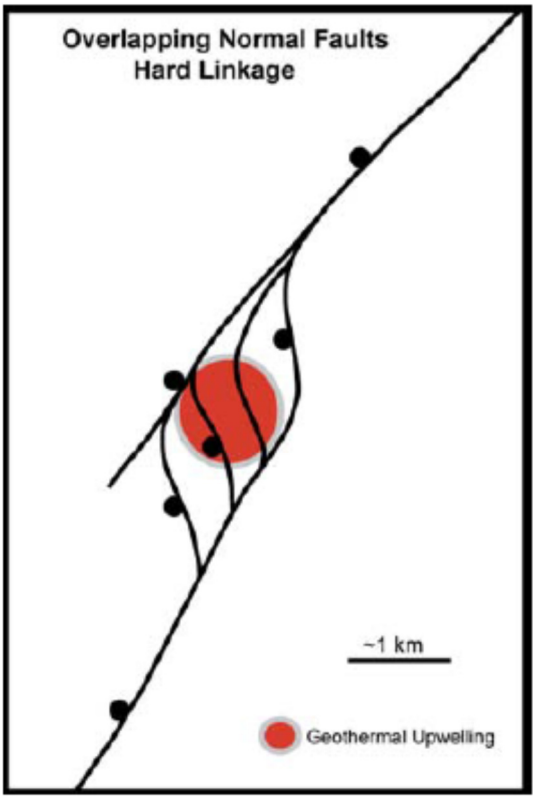

FIGURE 41: "Conceptual model of stepover in a normal fault zone. Multiple minor faults provide hard linkage between two major strands and serve to increase facture density, thus providing an avenue for the ascent of geothermal fluids." (Faulds et al. 2010)

A conceptual model integrates the data available from several geoscientific disciplines bringing together a consistent interpretation of all this data. Such a conceptual model provides a clearer rationale for well targeting, and furthermore one that can be tested – depending on the exploration results the model may be supported, modified or refuted. A good conceptual model has a number of qualities.

1. It should not be unnecessarily complicated. The simplest model that fits the available data is the best. Any additional complexity merely introduces spurious detail, since there is no data on which to base further specification. Elaboration can always be added later if new data do not fit the simpler form. This new data may indicate the nature of the changes that should be made.
2. It should not be so simple that essential characteristics of the system are dropped from consideration.
3. It should not be biased, for example, by fitting one specific data set with great accuracy while ignoring other information. For a flow model, chemical or enthalpy variation is just as significant as pressure variation. A conceptual model that describes one body of data at the expense of others is unlikely to be totally valid.
4. It should, where possible, fit observed rather than interpreted data. The latter may have already assumed some particular model and hence bias conceptualisation toward that model.

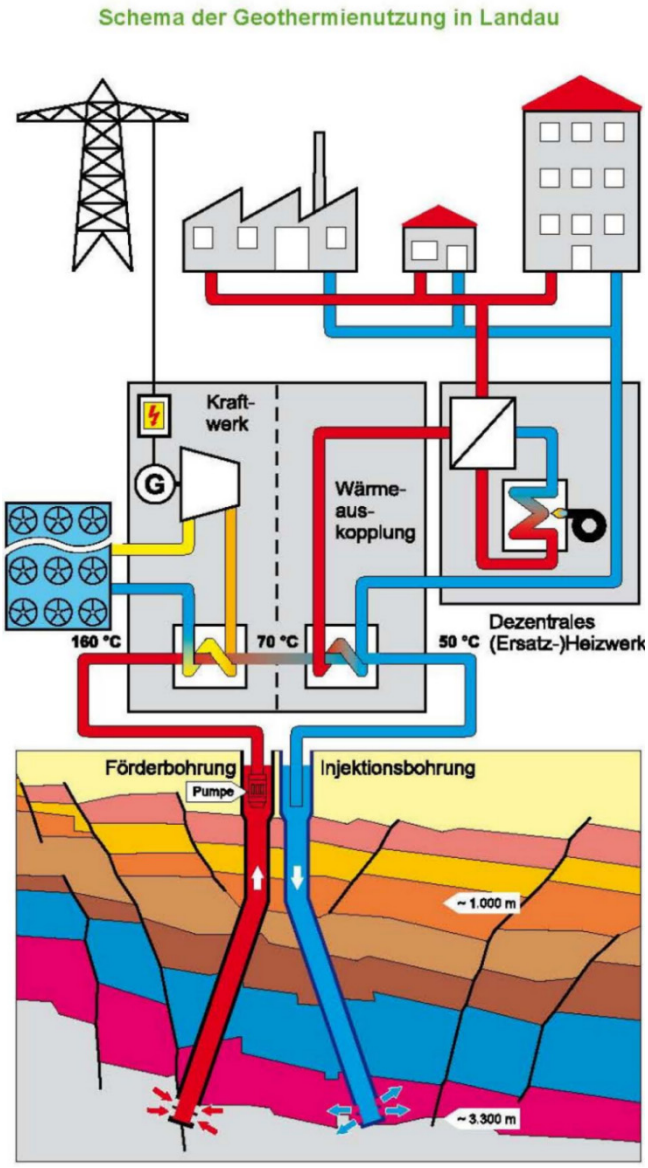

FIGURE 42: Landau, Germany

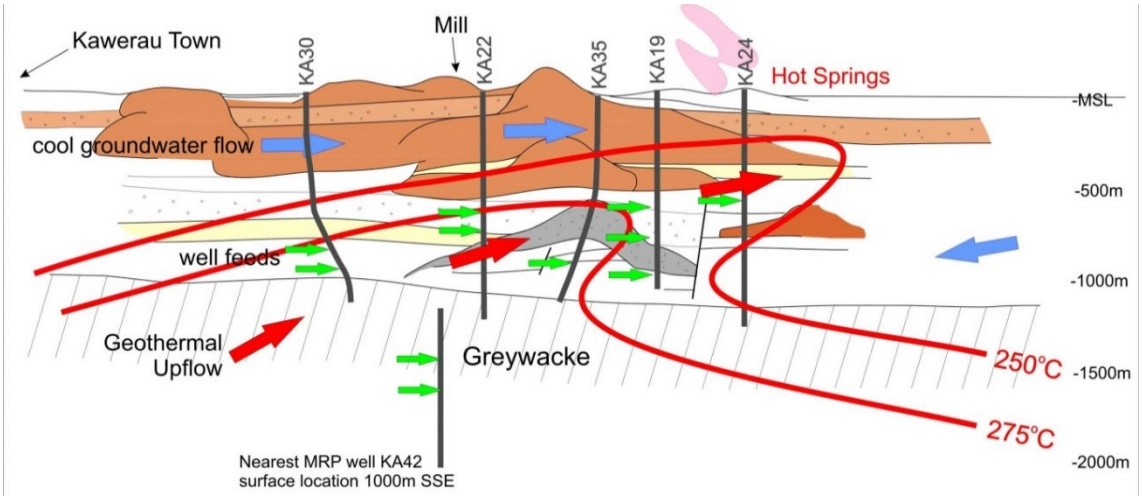

FIGURE 43: Conceptual model of Kawerau geothermal field

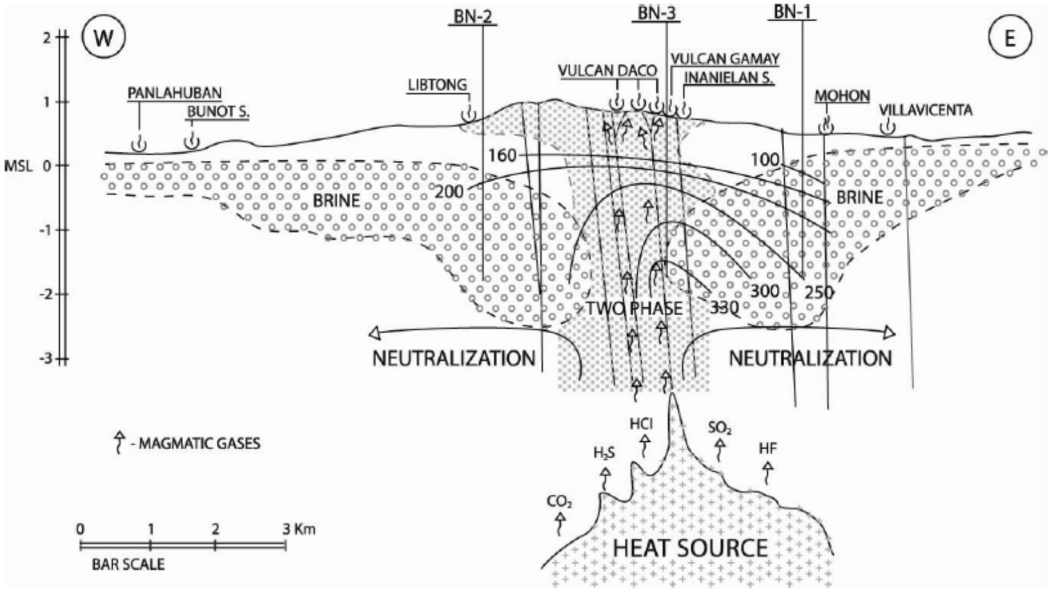

FIGURE 44: Vulcan-Libtong area (Apuada et al. 2010)

Not all of these requirements can be met with every model. Each geothermal field has its own individual characteristics and its model has to be viewed in that light. Conceptualisations can depend on unrecognised assumptions as well as observed information and will ultimately be checked only by long-term observation of the field. To the field developer the model that in the long term best matches the performance of the well field is best.

2. MAPPING THE RESERVOIR

The first conceptual models are constructed by the exploration geoscientists – geologists, geophysicists and geochemists. Reservoir engineering has little to contribute until wells have been drilled and tested, although there have been simulations of undrilled fields to verify that a proposed conceptual model could produce the observed surface signature.

The first step in conceptual modelling is to assemble the available data in a readily usable form. Typically this comes as maps, cross-sections or 3D computer visualisations of the data. Early in the exploration stages there will be geological and geophysical maps, and maps of surface thermal activity. Once drilling starts there is additional data from the wells and well tests. This data must be collated into a convenient form to show any patterns that may exist (for example by plotting the permeability onto the geology), and any anomalies that appear need to be checked or confirmed. Because these early descriptions can exert a strong influence on later interpretations, the mapping process is a very important phase of the reservoir analysis.

Figure 45 is an example conceptual model. The paper is about the High Temperature Zone (HTZ), so the most important information is the top of the HTZ and the top of steam (top of the normal reservoir). Also of interest is the hornfels (greywacke). At one time this was considered to be a marker for the reservoir bottom.

The following are some of the properties that might be mapped:

The reservoir geology
Surface and downhole geophysics
Reservoir temperature
Reservoir pressure

Permeability distribution
Zonation within the reservoir – liquid, two-phase or steam zones
Fluid chemistry
Natural discharges
Hydrothermal alteration
Well discharges
Surface deformation

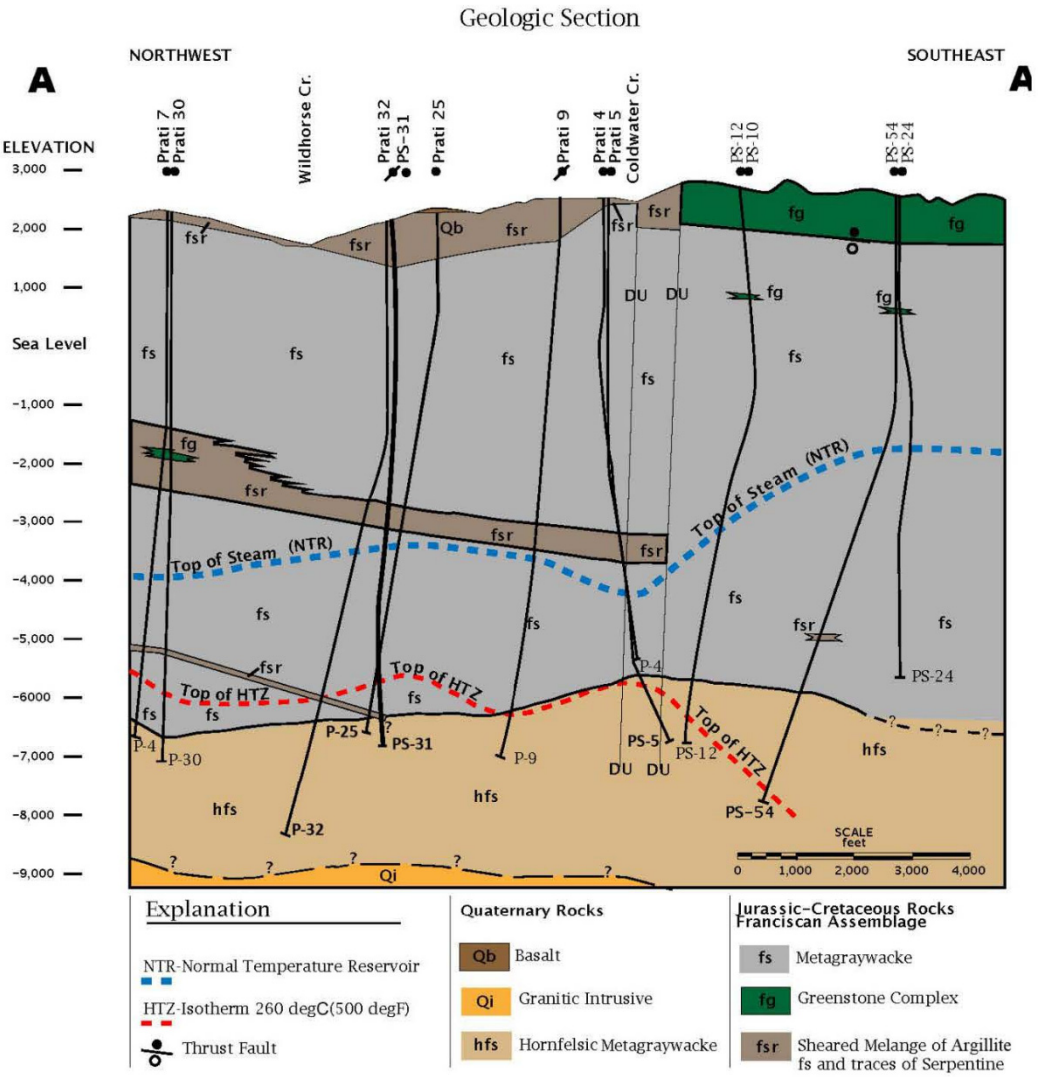

FIGURE 45: Geysers section (Lutz et al. 2012)

The list is not complete, and not all these points are used in any particular field. Deformation of the ground surface, for example is relevant only in an exploited field. These maps are normally not only contours of actual measurements, but will also use interpreted or summarised data. This implies some sifting of the data, usually based on judgements as to what is relevant. These judgements will change with time and revision is necessary as new information becomes available. Occasionally a new interpretation will cause a search through old records to check or reinterpret old data.

The reservoir engineer assembles data from the wells – reservoir temperature and pressure and permeability. The temperature is probably the most important of these data and when sufficient wells have been drilled isothermal maps of the reservoir can be prepared. Isothermal maps are useful in understanding the subsurface processes observed by different disciplines: the geologist may look for see correlation with structures and alteration, the geophysicist to see if resistivity correlates with

temperature, and the chemist wants to locate boiling, deposition or mixing processes. Because the isotherms imply the direction and location of the natural flow, and the location of economic reserves, they have a very strong impact on possible reservoir models.

The reservoir engineer therefore must provide the best estimates of reservoir temperature. If flows in the well mean reservoir temperature is not known in some interval, that lack of information must be reported. If the well is not fully heated so that only a minimum estimate of reservoir temperature is available, that must be reported. Temperatures outside the reservoir are as important as well as those within in it. These peripheral temperatures help define the field boundaries, and will be important in the later simulation, and can directly imply permeability or its absence.

The location of significant permeability within a well is probably next most important factor. The geologist, and other specialists, will be looking for any pattern in the location of permeability, or correlation with geological structure, in order to guide future drilling. Pressure is of interest to the reservoir engineer and the modeller. If there is a measurable pressure differential horizontally, or differential from static vertically, and natural flow is known, there is a direct measurement of permeability times the cross-sectional area of the flow.

3. TEMPERATURE PROFILES

Temperatures are easily measured and, with care, readily interpreted. A reservoir temperature profile may be determined by measurements in any well as it warms up after drilling and is discharged. Plotting these temperatures in plan view or section produces isothermal maps, perhaps the most basic representation of any aspect of a geothermal reservoir.

These maps immediately indicate the convective or conductive nature of the reservoir. Some inferences about the natural flow patterns are immediate. A natural hot recharge inflow must enter the reservoir at its hottest point and move toward cooler zones. A temperature reversal similarly implies a flow of colder water entering the reservoir. A zone of constant temperature implies convective mixing of fluid. In all cases, maximum or minimum zonal temperatures imply some flow and hence some permeability. However a thermal feature need not imply a large permeability. Convection so dominates conduction as a means of heat transport that even a small flow, in a zone of small permeability, can produce a major thermal feature. Generally once exploitation starts the subsurface flow pattern generated by exploitation overwhelms the natural flow. Changes in reservoir temperatures reflect changes in the reservoir as water boils or cooler water sweeps in. Note that there is no inference that recharge under exploitation enters the reservoir at its hottest point.

In an undisturbed field the vertical pressure gradient can be inferred from the pattern of the natural flow. For the effect on well profiles, there are three significant cases (and many more complicated special cases):

The upflow area of the field where the reservoir pressure gradient exceeds hydrostatic and the wells often contain upflows from a deep zone to shallower zones.

The outflow area where the fluid flows horizontally or nearly so, and wellbore pressures are close to equilibrium with the formation. In this part of the reservoir there is often little flow within the wellbore and consequently wellbore temperatures often reflect true formation conditions over a substantial depth interval.

The outflow area where hot fluid moves out over colder zones. Usually the hotter fluid is slightly overpressured and wells typically have downflows.

In an exploited field the past pattern of fluid withdrawal and injection determines the pressure distribution, which can be far from static.

3.1 Upflow conditions

The most common type of profile observed in the upflow area of a field is a boiling point profile: the well contains liquid water which for a significant interval is at boiling point, for pressure. This reflects an upflow in the well. Water enters the well, flows up and boils, and then exits higher up the well. The flow is relatively small so that the pressure profile never deviates from hydrostatic.

A second and more striking type of internal flow is the boiling crossflow, when the well contains fluid with a pressure gradient intermediate between water and steam. The profile is like that of a discharging well, and for the same reason. Steam and water are flowing up the wellbore sufficiently rapidly to mix and produce the typical intermediate pressure gradient. The flow must be sufficient to move the flow regime in the well from bubble to slug. This is a more vigorous form of upflow than the boiling point profile, which is a flow in bubble regime.

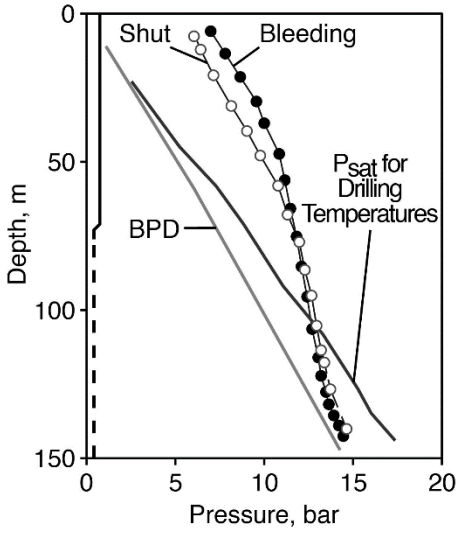

FIGURE 46: Profiles in Y-13, Yellowstone Park

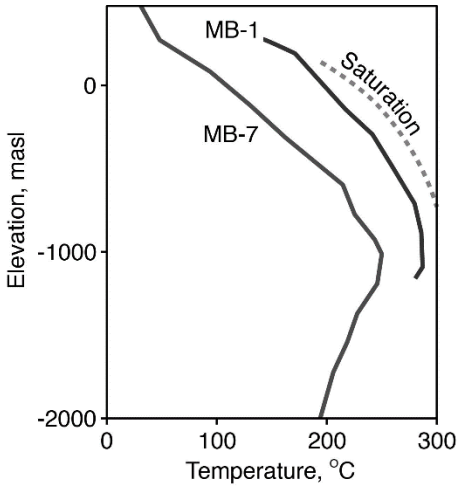

FIGURE 47: Stable temperatures in MB-1 & MB-7, Tongonan

Figure 46 shows a good example, well Y-13 at Yellowstone National Park. Temperatures were measured during drilling, and the corresponding saturation pressures are plotted. Note that the reservoir pressure gradient exceeds hydrostatic. The stable downhole pressures are also shown, both shut and bleeding. There is an upflow of boiling fluid in the well with pressure gradient less than hydrostatic, which exits into the formation at a shallow feedzone. Above the feedzone the pressure gradient is close to hydrostatic, so there is apparently water balanced on top of lower-density fluid. Such a profile is only possible because it is dynamic, not static. With the vigorous boiling upflow, steam rises into the casing. The casing is heated extremely rapidly and gas pressure (left after the steam condenses) builds up if the well is shut. The gas pressure will rise until it is bled off or the water level is depressed to the shallowest feed so any further gas is lost into the formation. The gas content of the reservoir need not be high to create a high gas pressure at wellhead – gas is concentrated in the casing by this process of distillation.

The presence of a boiling interzonal flow normally indicates that the well discharge will have significant excess enthalpy. Note that the low pressure gradient in the well does not indicate the same gradient in the reservoir. The reservoir gradient will usually be near hydrostatic, in an undisturbed reservoir. The reservoir gradient can only be determined by determining reservoir pressure at different depths, in different wells.

3.2 Static conditions

In the peripheral or outflow regions of the field, temperature profiles may show an absence of marked convective effects in the well. Figure 47 shows profiles in two wells from Tongonan, which penetrate the Malitbog outflow from the reservoir. The profile in MB-1 is similar to a boiling-point profile, but colder.

The reservoir fluid here derives from boiling fluid, which has flown laterally outward, cooling somewhat as it does so. The absence of marked convective effects in a well with good permeability indicates genuine equilibrium between well and reservoir – the reservoir is vertically hydrostatic. MB-7 shows an outflow with a temperature reversal.

Sometimes most or all of a field development takes place on an outflow. Examples are Ahuachapan, Yangbajan, Rebeira Grande, El Tatio, and the early developments of Wairakei and Kawerau. Exploratory drilling found excellent production on an outflow and development was based on this productive area. Only later is the upflow drilled and sometimes it is less permeable than the outflow region.

3.3 Downflow conditions

Like an upflow, a downflow is recognized by a near-isothermal profile. The water flowing in the well may gain or lose some heat conductively, so it heats or cools a little as it flows. Sometimes it is possible to recognize the existence of a flow in a well but be unable to decide whether the flow is up or down.

3.4 Conductive or cold water layers

In many places the upper layers above the high temperature reservoir may be quite cold. While in the area of surface discharge hot or boiling conditions may extend to surface, such activity normally occurs over only part of the field. Away from the surface activity, varying thicknesses of cold rock may be drilled. Two forms of temperature profiles are often found in such regions: a linear conductive gradient indicating poor permeability, and roughly isothermal cold temperatures, or large temperature inversions indicating cold aquifers – such cool aquifers usually have strong correlation to specific geological formations.

Figure 48a shows an example of the first, in well NM6 at Ngatamariki. The reservoir top is at 1800m, below which there is a low temperature gradient. Above this depth there is a region of roughly linear gradient to 500 m, interrupted by an aquifer at 1000m. Above 500 m are cold aquifers. Figure 48b shows an example of the second, well BR31 at Ohaaki. This well lies toward the edge of the reservoir. The reservoir top is at 550 m. Above this is a very steep gradient to cold aquifers above 400 m. The steep gradient between 400 and 550 m implies low permeability at this depth, whereas above 400m there is must be fluid movement, and hence permeability, in relatively cool rock.

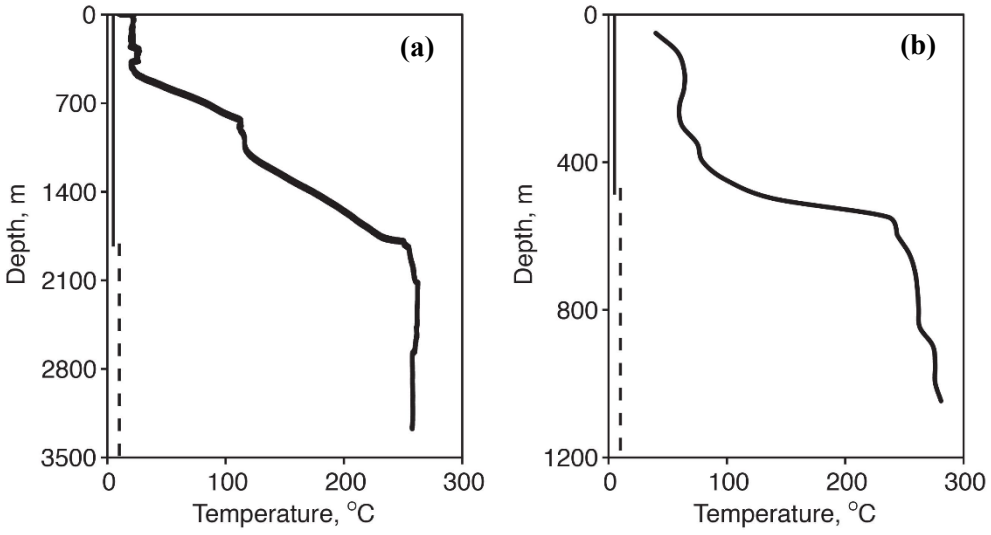

FIGURE 48: Temperatures in NM6 (a) & BR31 (b)

3.5 Rotorua and the ICBF (Grant, 1987)

Rotorua provides an example where inference was possible from the pressure distribution. Rotorua geothermal field in New Zealand has major surface discharge in the city of Rotorua, including geysers. It was also used extensively for home heating, with over 800 wells drilled. These wells typically produced from around 100m depth. By the early 1980s the surface activity was visibly declining. A program of monitoring was established, which produced the results shown here. The effects on the springs were so great that after a few years most of the wells were closed by government order.

The significant geological units are shown in Figure 49. The city of Rotorua covers the entire area of this figure. Below surface pumice and alluvia, wells find an ignimbrite layer. To the west of the city two there are two buried rhyolite domes. The wells normally find good permeability in the rhyolite or ignimbrite. There is a major structure, the Inner Caldera Boundary Fault (ICBF) in the south of the city. The major springs lie south of the ICBF.

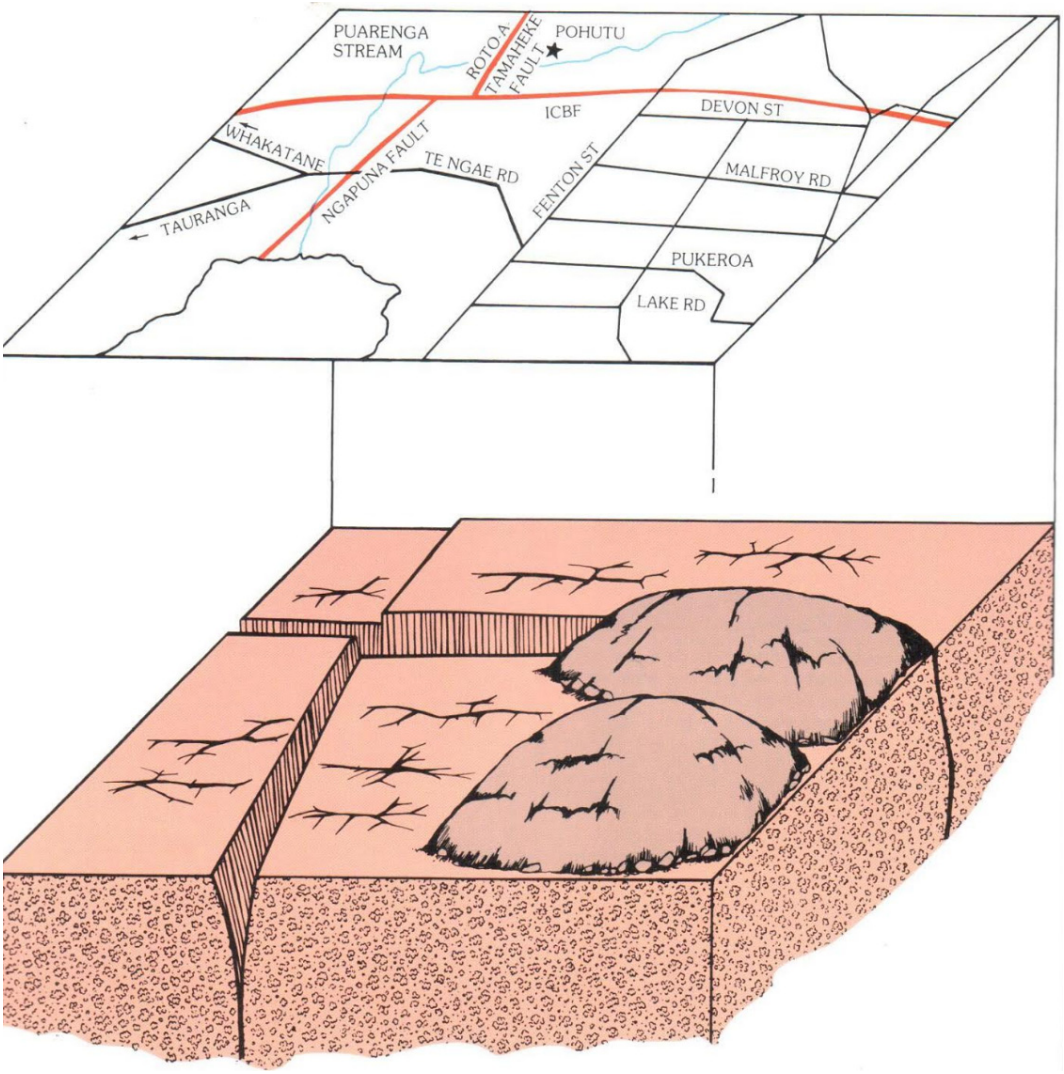

FIGURE 49: Sketch of Rotorua near-surface geology (vertically exaggerated)

Figure 50 shows the horizontal pressure distribution at a depth corresponding to the usual production depth of the wells. From this distribution two conclusions can be drawn. The first is that the difference between the rhyolite and the ignimbrite does not appear to matter so far as the pressure distribution is concerned. The second is that the ICBF does matter. There is a region of markedly greater horizontal pressure gradient that coincides fairly closely with the ICBF.

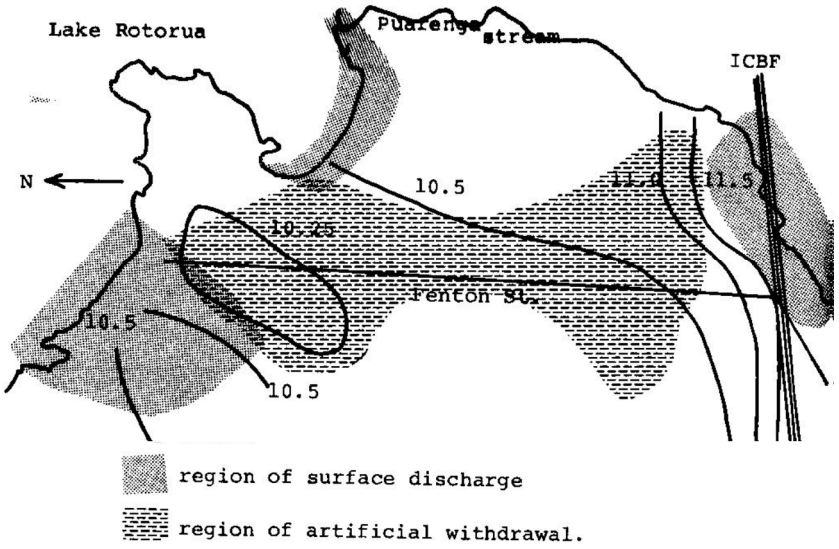

FIGURE 50: Pressure distribution at RL+180m (approx. 100m depth)

LECTURE 5

FIELD MODELLING

1. INTRODUCTION

This talk outlines the use of simulation by the reservoir engineer. The approach assumes that the reservoir engineer provides data to, and receives output from, another person who carries out the simulation. Sometimes one person performs both roles, of reservoir engineer and modeller/simulator. In this discussion only the reservoir engineering input is considered and the mechanics of carrying out a simulation is not discussed. For the simulator's viewpoint see O'Sullivan et al. (2001). The focus here is on what data is needed, the procedures for calibrating the model and what results may reasonably be expected.

The process is not a simple step of providing data and receiving results. One of the great advantages of a simulation is that it makes computations in accord with physical and mathematical laws: it is logically and internally consistent. In contrast, when constructing a lumped-parameter model it is possible to make simplifying assumptions that are not consistent with the system structure. Modelling, in theory, avoids this hazard by explicitly representing the known information. Often the process of model building shows that some data is not consistent or very difficult to fit, and requires review. This sends the reservoir engineer back to check on actual measured data and its processing and interpretation. Perhaps it is possible to cross-check the data against other measurements. Perhaps the interpretation was wrong. Or if the data is solid, then more work is implied for the modeller to make the model fit what appeared to be inconsistent data. Or perhaps the conceptual model requires revision.

2. INPUT DATA

Basic inputs for modelling are:

1. A conceptual model of the reservoir
2. Natural state pressure and temperature distribution
3. Well tests and interference tests
4. Production and injection history: mass flow, enthalpy/temperature and possibly wellhead pressure
5. Changes in reservoir pressure and temperature during production
6. Well specifications (locations of feed zones)

Other data which can be used include:

1. Gas and chemical distribution in natural state
2. Changes in gas and chemistry during production and injection
3. Changes in gravity during production and injection
4. Changes in surface elevation during production and injection
5. Changes in surface activity
6. Tracer tests
7. SP

In principle any physical parameter that is changed with fluid change, and is conveniently measurable, could be used, provided that there is a computable physical model to relate its change to the reservoir changes.

New parameters introduce new properties to be set. For example, modelling subsidence requires specification of the elastic properties of the reservoir rock. Matching subsidence is primarily about fitting these elastic properties, but the pattern of subsidence also reflects pressure changes in and above the reservoir, so that there is some constraint on possible reservoir pressure, and hence some additional

constraint on reservoir permeability and porosity. For example, there is often a broad pattern of subsidence across the entire reservoir – this pattern essentially outlines the area over which pressures have fallen, and so indicates the boundary of the area where pressure has fallen. Conversely, a localised area of subsidence implies compaction close to surface, so the reservoir model must have pressure or temperature change close to surface.

In general a model needs constraints, observational data of relevant physical parameters. More constraints improve the model by restricting possible models. At Wairakei lumped parameter models showed that different physical models produced identical fits to one data history, the field pressure. The models were separated by adding additional data, the possible physical size of the reservoir. Introducing a different type of data usually provides a different constraint on the model, affecting different parameters. For example the natural (steady) state of a reservoir depends only on rock permeability and not at all on porosity, while changes in enthalpy, gas or chemistry under production or during well testing in a two-phase reservoir are highly sensitive to porosity.

A model can be constructed at the exploration (pre-development) phase, using only natural-state plus well-testing (including interference testing) data. Such a model is partly calibrated. It provides some estimates of future reservoir performance under production but lacks the constraints provided by a production history. Porosity is little constrained, and the fitted permeabilities are dependent on measurements of the natural flow. If there is undetected subsurface discharge, the natural flow will be understated and the permeabilities underestimated. There is no constraint on possible stimulated flow from external aquifers which are in equilibrium in the natural state, as the strength of this connection is not tested by the natural state modelling.

The following sections discuss how the information which is collected by the methods of the previous chapters is used in the model construction and calibration.

3. CONCEPTUAL MODEL

The conceptual model is the first guide to the numerical model. This incorporates the mental models of the geoscientists working on the reservoir – the construction of a pattern from the mixture of physical information available. The reservoir engineering data is important – temperatures and pressures provide an indication of where fluid is flowing. The geophysics provides an estimate of the boundary of the reservoir, beyond the drilled area. Normally the model will start by assuming that the permeable reservoir extends across the area of geophysical anomaly, with permeability decreasing at the edges. The drilled wells or geophysics may or may not indicate a bottom to the reservoir. The geology provides the structure of the model. For a first assumption parameters, most importantly porosity and permeability, will be assigned to each geological unit. Any relevant structure such as a fault or formation contact can be incorporated as a region of higher permeability. If there is some regional trend or major structure it is usually more convenient to orient the model grid parallel to that trend, so that structures can be conveniently represented as a line of blocks or by changing the grid detail.

4. NATURAL STATE

The first step in model calibration is to match the natural state. The relevant data are the natural temperatures and pressures, and the amount of surface discharge, as both heat and mass. The reservoir model is constructed with an input of mass and heat at the bottom, possible infiltration from the surface, and leaks at sites of surface or subsurface discharge. It is then run until a steady state is reached. The temperature and pressure distribution is then compared against the measured data. Then some parameters are changed and the model re-run until a steady state is obtained which is closer to the observations. The process of adjusting parameters to get a natural state match is usually slow. As well as structure within the reservoir model the boundary conditions may be adjusted – a side boundary may

be impermeable or may allow contact to a lateral aquifer, the model bottom may be deepened to bring more of the region in which fluid flow is affected by production within the model.

It is important at least in the initial stages of development that the model structure be as simple as possible, but still contains within it the mechanisms that affect reservoir processes. For example, if there is a complex pattern of deep inflows, rather than one or two sources, this indicates that there is structure at greater depth influencing the flow pattern, which should be included within the model. If there are constant pressure boundaries (except at surface) that contribute significant flow under exploitation, this again indicates that an important assumed property of the reservoir has been located outside the model, and again the model should be enlarged so that nearly all flow is contained within the model.

It is important that the information used as input into the model is "real" – i.e. the pressure and temperature measurements must be carefully interpreted to provide best estimates of the reservoir temperature and pressure. Some data may turn out to be critical and this should be re-checked. Model structure is often sensitive to anomalous pressures, and it will need to be checked that an anomalous pressure genuinely is high or low.

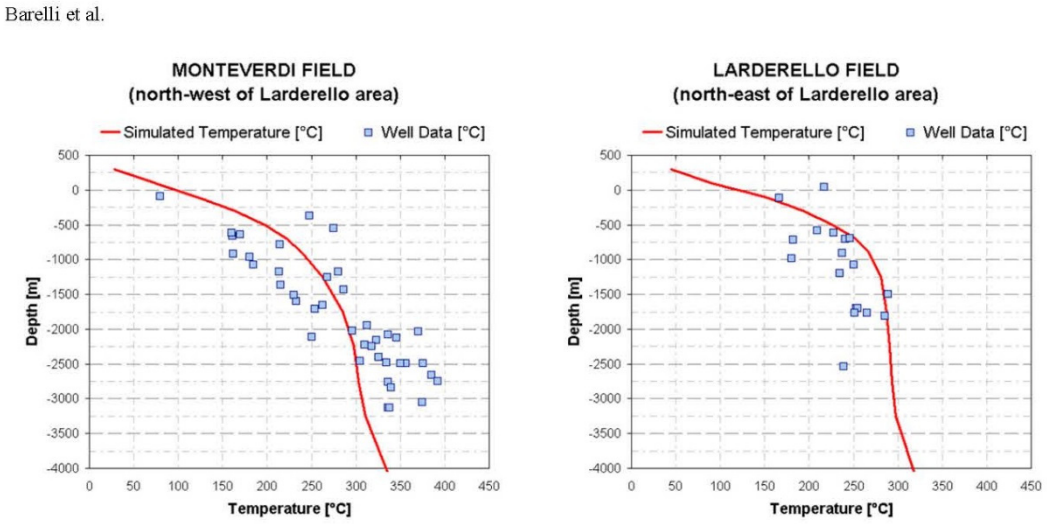

FIGURE 51: Simulation temperature match (Barelli et al., 2010)

Temperatures are best presented as well-by-well matches of interpreted well temperature values and model results. Data should be compared on a well-by-well basis as that is where the data is. It is useful also to have isotherms in maps or sections but as this involves some smoothing of the actual data it is not as accurate a calibration. Contours on particular layers can be helpful in visualising fluid flow in those layers.

Figure 51 shows a set of well temperature matches for Larderello. Hoang et al. (2005) show a pressure match in a vapour-dominated reservoir. Figure 52 shows the comparison of modelled against measured pressures at Ngatamariki. Each of these presents a comparison between simulated and observed data.

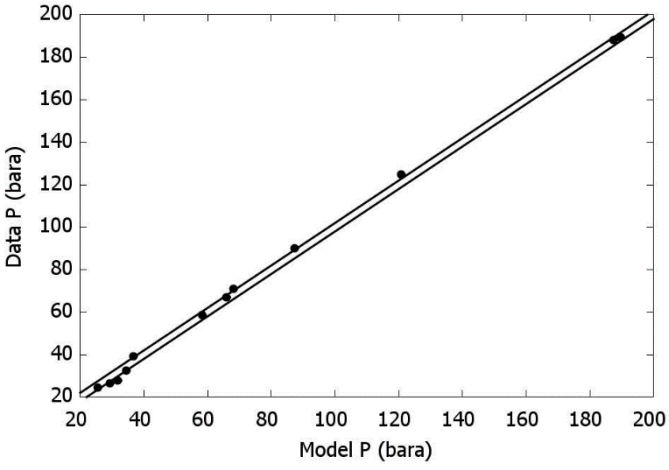

FIGURE 52: Comparison of measured and calculated pressures

Sometimes an explicit goodness of fit measure is used, usually some variant of the sum of the deviations or squares of deviations in pressure and/or temperature data, normalised by reference to some pressure/temperature. This provides a more objective measure of how closely the data has been matched than visual inspection. Visual comparisons are still needed to ensure that the simulated results have the right pattern.

It will normally take considerable time, adjusting permeabilities, to get an acceptable natural state match. Automated parameter matching can be done (using iTOUGH2) but only a few parameters can be matched at a time without greatly escalating computing time. There may be only a limited number of wells drilled before production, limiting the data defining the natural state. Often wells drilled after production has commenced are used, assuming that the temperature has changed little so that the later profiles are representative of the natural state profile. A more rigorous approach is to match the data from later wells with simulated data for the time of measurement, that is match the later profiles as a part of production matching.

Interference tests should be available at this phase of field development and can be used to provide additional calibration. The tests are normally analysed using standard uniform aquifer models to obtain transmissivity and storativity, which are then used as initial estimates for the reservoir in the area around the wells involved. When the interference deviates from a uniform aquifer, it is usually simplest to simulate the interference test with the model, and then adjust model parameters to obtain a best fit. The simulation will not get fine detail of the short-time interference correct, due to the block size, but it should get the larger and longer-time response correct.

5. WELL SPECIFICATION

Each of the wells in the field should have been fully interpreted to create a well model. If the simulator is coupled to a wellbore simulator, then the specification of feed depth(s) and productivity/injectivity of each feed, together with the well casing and deviation, provides a full specification of the well. The simulator provides the reservoir pressure and fluid quality at each feed and from these the wellbore simulator can calculate the well flow at specified wellhead pressure.

Most current simulators do not include a coupled wellbore simulator and it is necessary to make a simpler well specification. This may be an allocation of flow to different zones at fixed ratios, these ratios having been assessed at some flowing state that is representative of reservoir conditions for the simulation period, or use of a look-up table which is based on the results of wellbore simulations, or some other computationally convenient simplification. Total flow of the well is calculated by the simulator using a simple formula or look-up table, again defined from wellbore simulations of a representative flowing state.

The full detail of well specification may or may not be important to the simulation. If the reservoir is reasonably homogeneous and permeable, the detail of flow allocation may not be particularly important as the reservoir response is more controlled by the total flow, and well performance is not much affected by the depth of fluid entry.

In other cases detailed well specification is more important, particularly when there is significant stratification within the reservoir. One such case is when there is a two-phase zone over a deeper liquid zone. Well performance and discharge enthalpy are then strongly influenced by the proportion of fluid taken from the two-phase zone, and this in turn affects the power capacity of the production and design of plant. A second case is when there are cool zones within an otherwise homogeneous liquid reservoir, say from injection returns. This again affects, adversely, well performance and discharge enthalpy, and in turn power capacity and plant design.

6. HISTORY MATCHING

Once the natural state matching has been done, wells are specified and the model is then used for production runs, to simulate the changes under exploitation. The simulated changes are compared with actual measurements, and another cycle of parameter adjustments made to generate a fit. The parameter changes also affect the natural state model so it is necessary to re-run the natural state to make sure this match has not been degraded. Further iterations may be needed to get acceptable matches to both the natural state and production history.

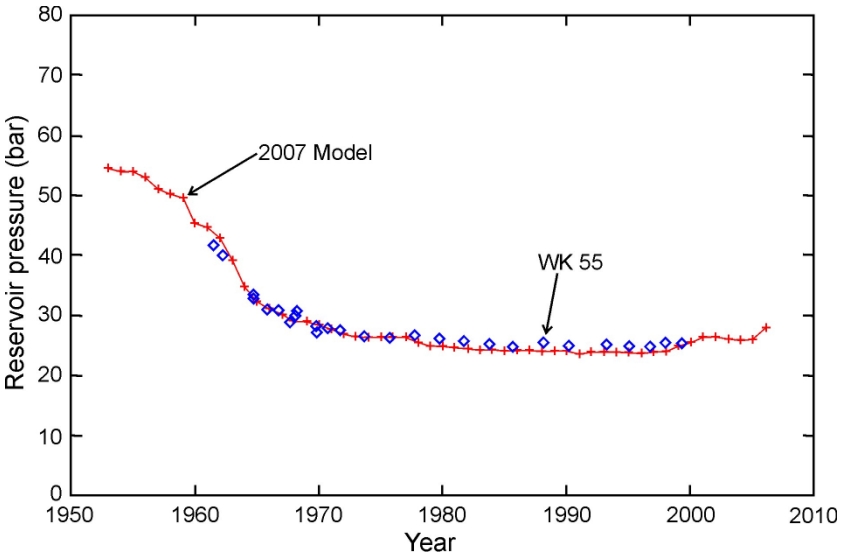

FIGURE 53: Pressure history match

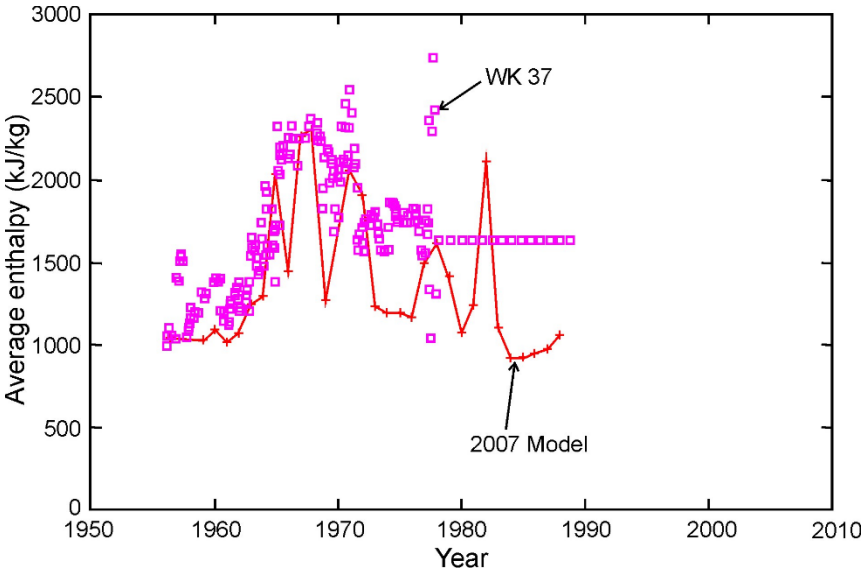

FIGURE 54: Enthalpy history match

The following figures (Figures 53-55) show history matches from the Wairakei-Tauhara model of O'Sullivan et al (2009), matching pressure in one well, enthalpy in one well, and surface heat flow. These are only a sample of the data matched, as many well pressures, and enthalpies, were matched, giving a match to data across the field and its history.

Earlier models of Wairakei tended match the average field pressure, as pressure is fairly uniform across the field. Later models match specific well histories, thereby ensuring a match to the distribution of pressure across the reservoir as well as with time (Figure 53). Figure 54 shows a match to the average enthalpy of one well. As Wairakei developed a steam zone with drawdown, well enthalpy depends on the depth of feed zones. To get an accurate match it is necessary to have an accurate representation of the feed depths, so that there is the correct proportion of fluid taken from steam and water zones; and an accurate simulation of the process of vertical drainage and segregation, which tests the vertical permeability. The match to surface heat flux, shown in Figure 55, requires fine structure in the shallow layers of the model.

With the development of the steam zone there came a large increase in surface heat discharge, which early models did not match. Making a model match required calibration of the shallow model layers and finer layer structure near surface. These changes have little direct impact on reservoir performance, but are critical for calibrating the model representation of surface and near-surface changes, which are increasingly important for assessments of environmental impact.

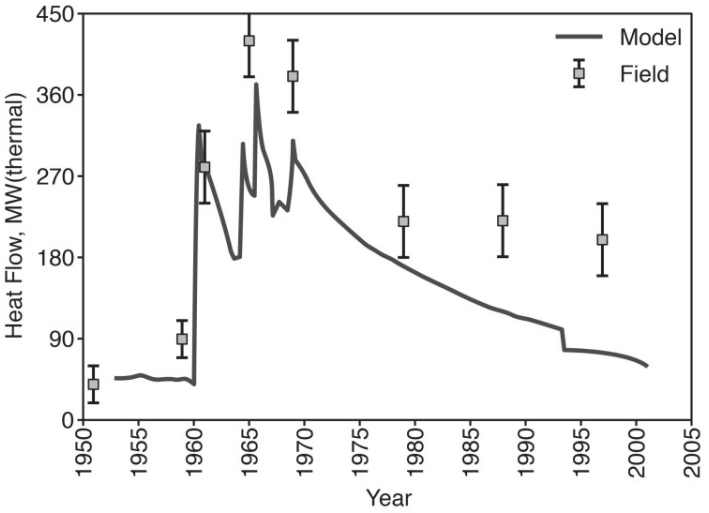

FIGURE 55: Surface discharge match

Figure 56 shows a history match, from the model of Hatchobaru in Japan (Tokita et al. 2000). The model matches a range of data, tracer, pressure, temperature and gravity. Matches to such wide range of data provide considerable constraint to the possible reservoir structure, and provides increased confidence in simulated outcomes. In the case of Hatchobaru thermal interference from injection returns is a management problem, and the simulation, by matching both temperature changes and tracer returns, is calibration of the parameters critical to this interference.

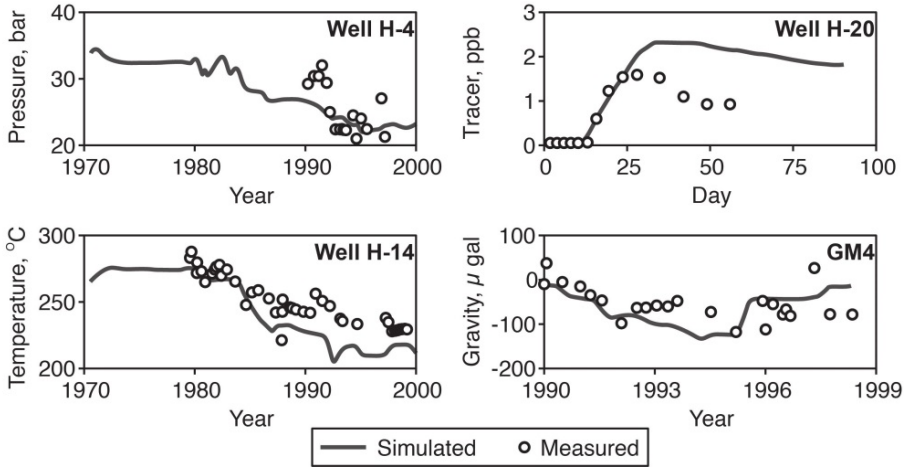

FIGURE 56: Hatchobaru model matches

7. CALIBRATION

How the actual calibration is carried out and presented has an important impact on the quality of the result. The simulation has to fit a range of different data of different character and quality and the appropriate calibration criteria may not be obvious. There are methods used that range from good to unacceptable.

7.1 Good

If automated fitting is used, this is done by defining an objective function. This is usually something like the sum of the deviations, or deviations squared, over a range of datum points. At each point there is an observed value, and a simulated value. The fitting algorithm tries to find the simulation that minimises these deviations.

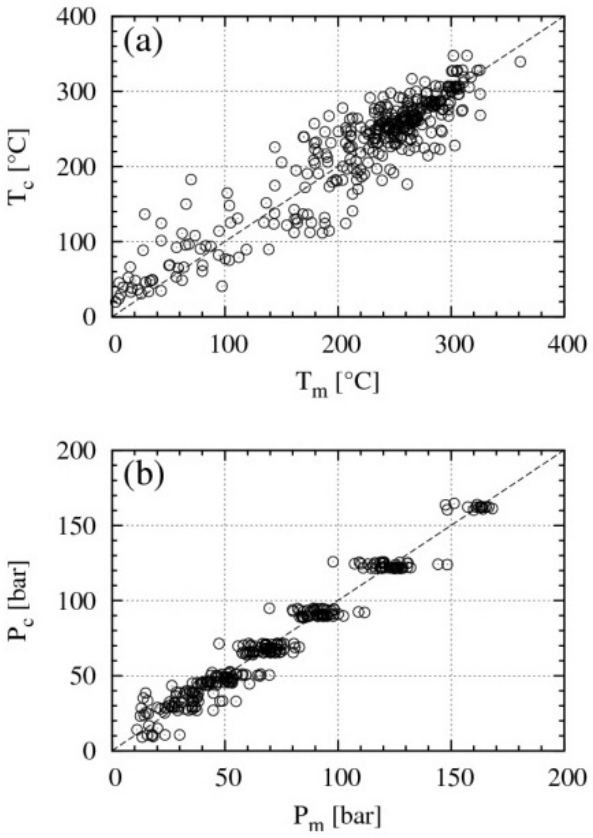

FIGURE 57: Comparison of measured and calculated values of pressure and temperature (Gunnarson et al, 2010)

It is also necessary to have a criterion as to how close a match is required, and this can vary with the case. In a reservoir that is entirely liquid, the absolute pressure is not very important and only pressure differences matter. But when there is boiling present, the absolute pressure matters as it determines where there is boiling.

It is important to use as wide a range of data as possible, and generally better to have a fit that is moderately good over such a wide data set rather than a close fit to just one set of information. For example, it is often easy to fit a pressure history but many different models will produce similar pressure histories. To further discriminate between models requires the introduction of a wider range of data.

As it happens, this is also the best way to undertake manual calibration, but it may not be presented in precisely this form. Figure 57 and 52 show examples where simulated and measured data are compared. Another way to do this that is not seen very often is to present the residuals – the differences between measured and simulated values, plotted against a relevant variable such as time, depth or location. This has the advantage of showing up any systematic pattern in the residuals. Figure 58 shows a plot of residuals in a pressure-transient fit. There is clearly a systematic pattern in the residuals, which suggests what sort of modification is needed. If the residuals simply showed a pattern of random noise this would imply that the model was as good as possible, with this data.

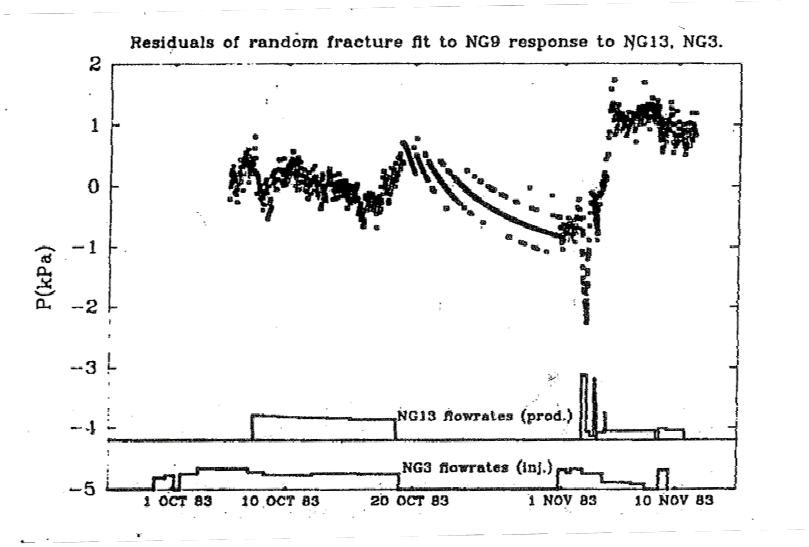

FIGURE 58: Residuals of fit of pressure transient model for Ngawha interference test (Grant & McGuiness 1985)

Also good is a direct comparison of simulated and observed data. For history matching this is usually the only easy way.

Figure 59 shows a history match. Note that the match is visually pretty close – at this scale the data is, to visual appearance, pretty well overlying the model. One can only judge the accuracy of the fit by the coefficient of determination. There are actually three models shown but visually they are all good. It is only the actual coefficient values that discriminate between

them. The visual comparison does not discriminate between the fits, but the coefficients show the 3-tank model is significantly better.

It is important to present data in such a way that it is clear where the actual comparison is made. The observational data exists only at discrete points. For pressure data this is one point per well, for temperatures several points per well. In the plot, Figure 59, the simulation is represented by the line and the data by the actual datum points. The simulation data of course also exists only at discrete points, namely the midpoints of the blocks, and is interpolated between them. When pressure data is being compared, the observations exist at the well feed points. The simulated data exist at the block centres and it is necessary to interpolate between these latter to provide a direct comparison with the data.

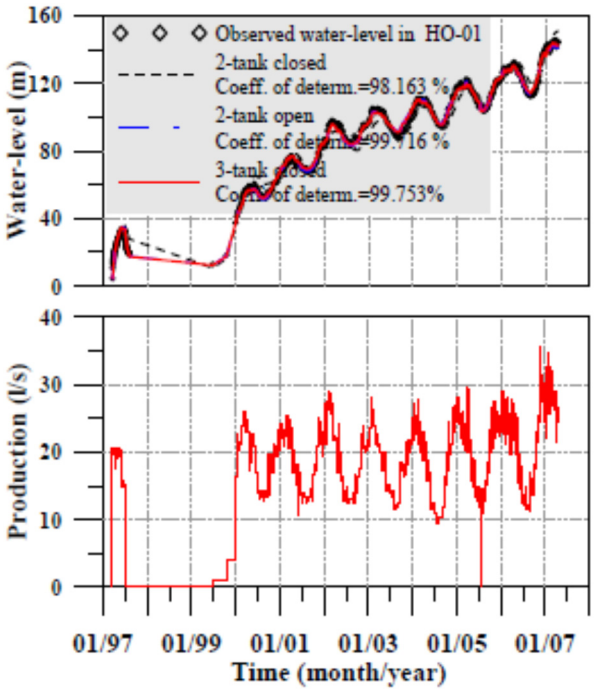

FIGURE 59: History match (Guo et al 2010)

7.2 Useful

The next method of comparison is to make contour plots and compare these. Figure 60 shows measured and simulated formation temperatures. Isothermal plots such as these are good for showing patterns – it is possible to see if the simulation has the hot spots in the right places, the right sort of outflow, and so on. However this is a poor way of judging the quality of the fit, and the direct data comparison of Figure

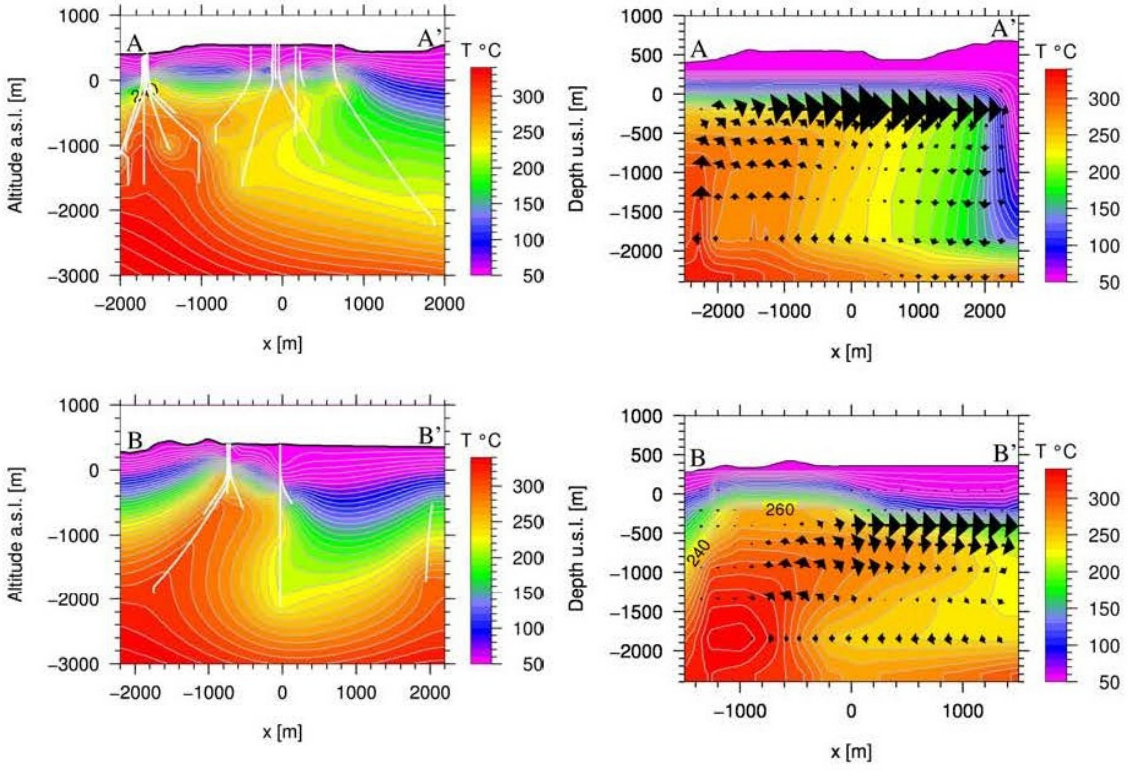

FIGURE 60: Formation temperatures, measured and simulated (Gunnarson et al. 2010)

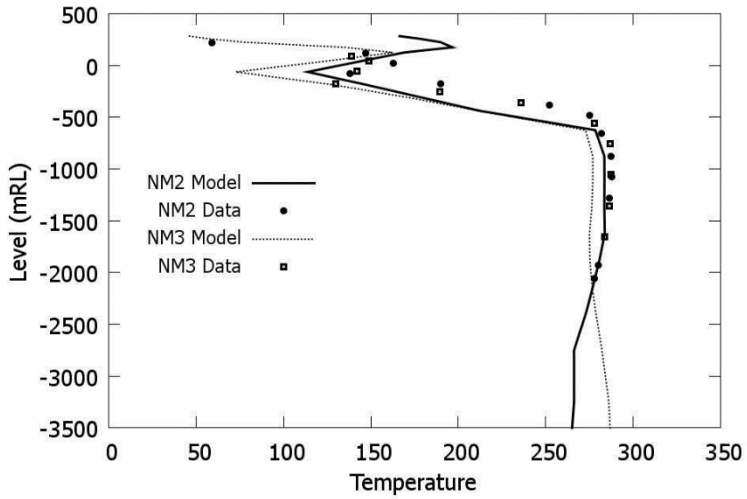

FIGURE 61: Temperature calibration

57 is the only way to measure the quality of the fit. In addition there is the problem that the isotherms have been extrapolated well beyond the region with data.

Temperature calibrations (Figure 61) are properly shown by comparing the data, as in Figures 57 or 51. The temperature data measured in the wells is all the temperature data there is. If the model fits those data it is fitting. The isotherms introduce additional elements and are a mixture of data and interpretation.

There is one aspect where consideration of the isotherms can be helpful. If most of the wells are in one location, fitting the downhole profiles means that this location is over weighted. Inspecting the isotherms tends to weight all areas equally. However this problem of overweighting a group of wells can be simply dealt with by weighting the other data more heavily in the computation of residuals.

7.3 Unacceptable

Sometimes the match is presented as a direct comparison of isotherms, as in Figure 62. This does not provide a good representation of the quality of the match. What is not presented is where the observed data are. The isotherms are constructions from the data, and contain a mixture of data and interpretation. It is also not possible to see clearly how large the deviations are.

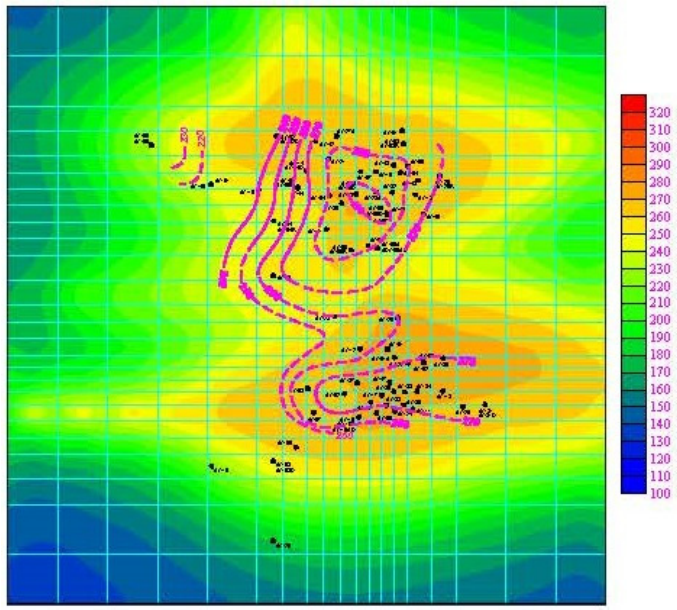

FIGURE 62: Measured and simulated isotherms

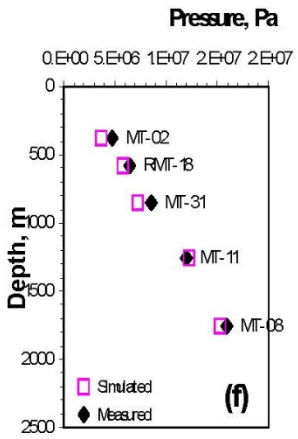

FIGURE 63: Pressure compare-son, measured and simulated

Also not good practice is a comparative plot of pressure against depth, as shown in Figure 63. Both measured and simulated pressures increase roughly hydrostatic with depth, which means that the pressure scale is quite large. Any simulation is going to produce a pressure roughly hydrostatic with depth. It is very difficult to see how large the deviations between the two are. This does not present the data clearly, as in liquid-dominated systems all the well profiles are normally

hydrostatic and the differences between wells small compared to the total pressure, so that it is difficult to judge if the simulation correctly represents the relatively small deviations from hydrostatic equilibrium. Even worse is a plot comparing downhole pressure profiles against simulated pressure profiles, as in Figure 64. The measured data is the measured downhole profile, whereas the simulated data is the simulated reservoir pressure profile. Showing the two profiles is nonsense – they are only comparable at one point, the well's feedpoint. That isn't identified. Even if it were, the problem of the scale means it would be very difficult to tell how close that one datum was to the simulated profile.

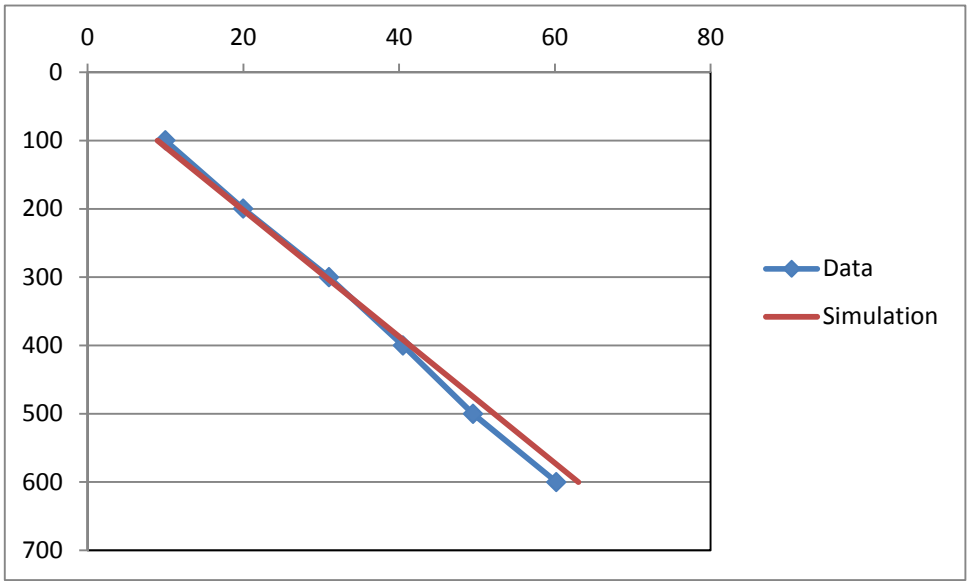

FIGURE 64: Wrong way to show pressure match (synthetic data)

7.4 Acknowledgement

Thanks to J. Burnell for reviewing.

LECTURE 6

KAWERAU GEOTHERMAL FIELD

Kawerau is located in the Taupo Volcanic Zone, in the North Island of New Zealand. Figure 65 shows its location.

Kawerau is the world's largest direct heat use of geothermal. The field has been developed to supply steam, and later power, to a pulp and paper mill. Field development has therefore been relatively slow, depending upon the mill's demand. Figure 66 is a view over the field in 2012, taken from Putauaki, the volcano on the field's southern edge. There is extensive industrial development, which constrains drilling and pipelines. On the right there is the 110MW power station developed in 2008. The town lies off the left edge of the image.

The field history can be divided into five phases:

- Phase 1: 1954-1959
- Phase 2: Repair 1960-1966
- Phase 3: Exploration
- Phase 4: Maintenance
- Phase 5: Expansion in 2000s

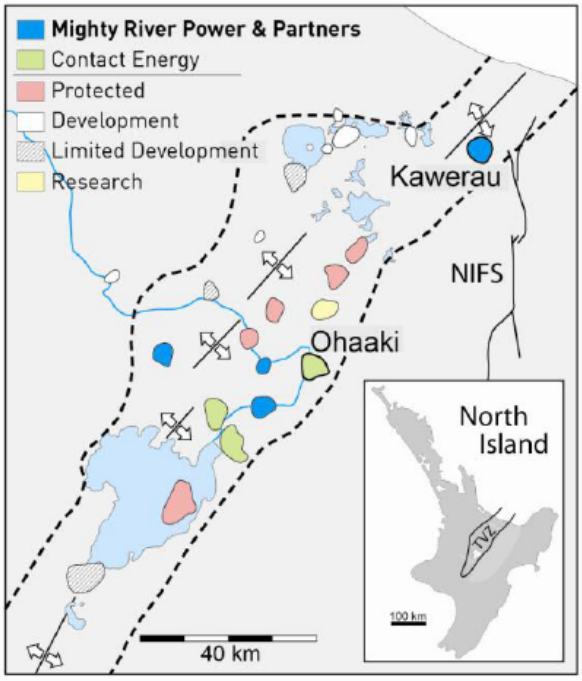

FIGURE 65: Location of Kawerau geothermal field

FIGURE 66: View across Kawerau

1. PHASE 1 – THE 1950S

Figure 67 shows the wellfield developed in the 1950s.

FIGURE 67: 1950s development. Note that the background photo is from 2005

There was at the time no idea of the field's extent. Wells were drilled (by a water well driller) to a depth of up to 500 m, near the springs. Some of the wells were successful, and the pulp mill was planned lying south of these wells. Wells KA1-14 were drilled in this period. All produce from volcanics.

The wells turned out to have a short lifespan. There was some initial excess enthalpy, but wells rapidly quenched and production failed by 1959. Documentation and measurements are sparse from this period.

2. PHASE 2 – REPAIR

The Wairakei geothermal drillers and field crew were used to rehabilitate the wellfield. Many of the wells had broken or insufficiently well cemented casings. Some wells were repaired, with varying degrees of success. Some wells were deepened, again with varying success. Some wells were abandoned. The total result was to restore sufficient production for the mill. Production mostly now came from the depth interval 500-800m, in various volcanic rocks.

There was also an assessment of the field by Banwell, who observed that cold water incursion was a significant problem. There was little if any drop in reservoir pressure, and well permeability was often very good. Well KA8, after it was deepened, was the largest geothermal well in NZ.

The first resistivity survey was done in 1970. This survey is shown on Figure 68.

The resistivity indicated that the field was significantly larger than the area so far drilled, extending further to the south-west.

Wells KA16, 17 and 19 were drilled as makeup wells in the late 1960s, and KA21 in 1975. KA19 was then the largest geothermal producer in NZ, until it was supplanted by KA21. KA21 was of interest also because it penetrated greywacke beneath the volcanics, and found excellent permeability in the greywacke.

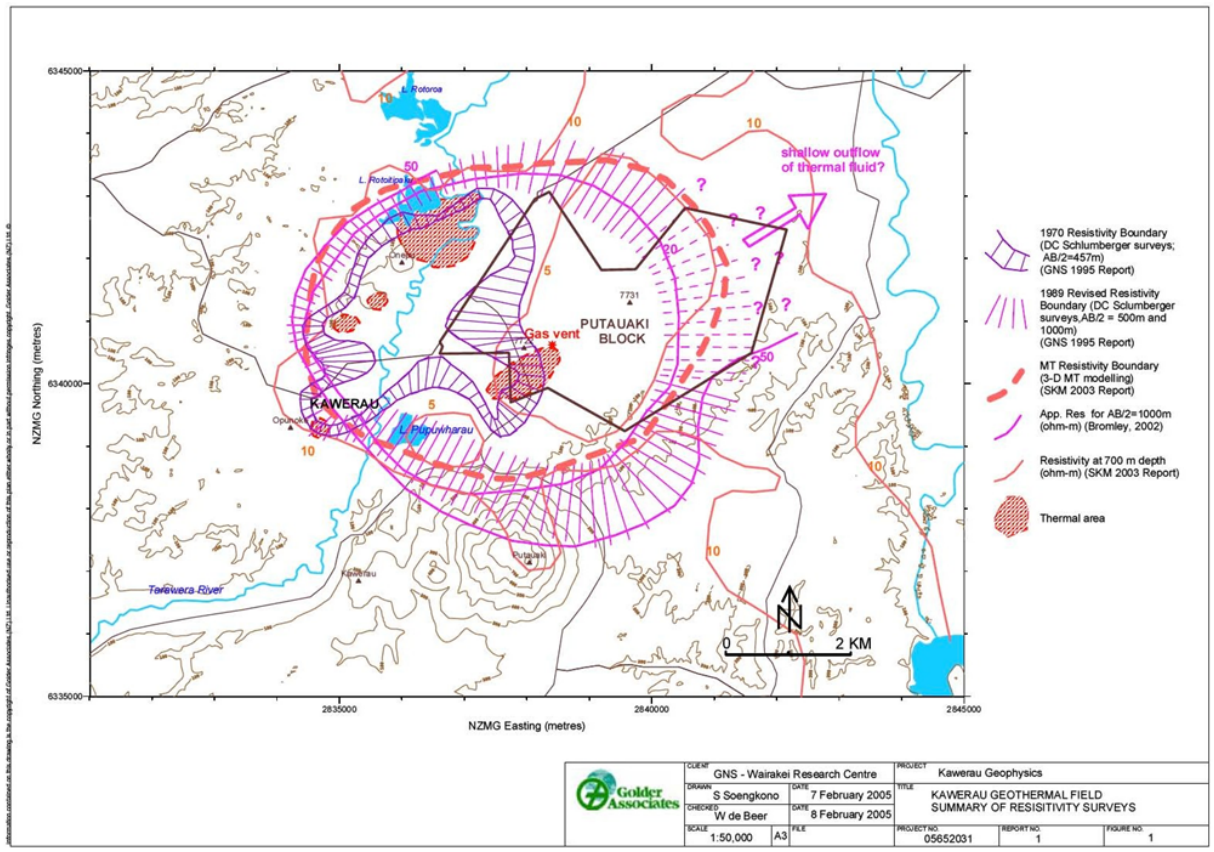

FIGURE 68: Kawerau resistivity surveys

3. PHASE 3 – EXPLORATION

From 1975 to 1985 wells KA21-35 were drilled, providing a scatter across the field area as shown by the 1970 resistivity. Figure 69 shows the wellfield after this drilling. Some wells were successful (KA22, 24, 27, 28, 30). By contrast KA23, 26 & 29 found high temperatures but poor to very poor permeability. Maximum depth of these latter wells was only a bit over 1000m. It is not clear why this exploration was undertaken, as there was no need for additional mill supply and no plan for other use such as electricity generation. One interesting result was KA31, which had a cold (96°C) inversion despite being in the centre of the field. This has been presumed to be a consequence of cold incursion rather than an original feature, as shown in Figure 70.

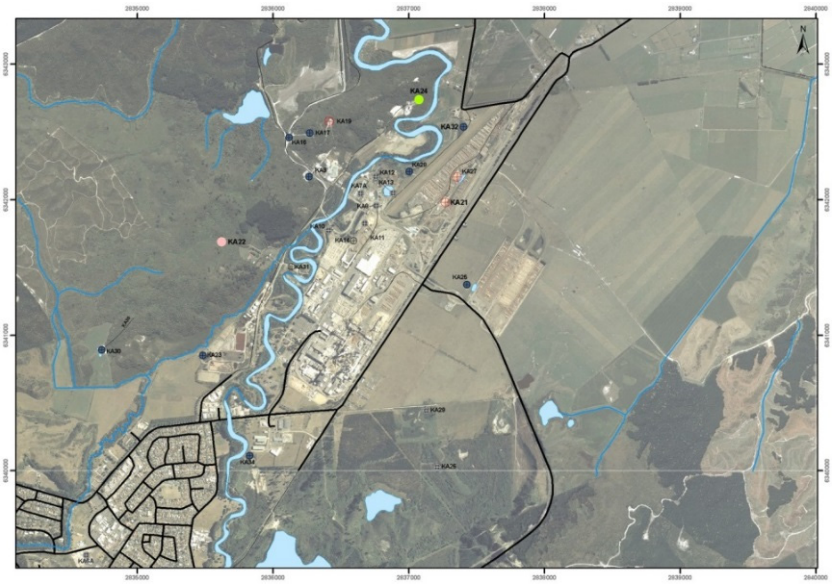

FIGURE 69: Kawerau wellfield after KA32

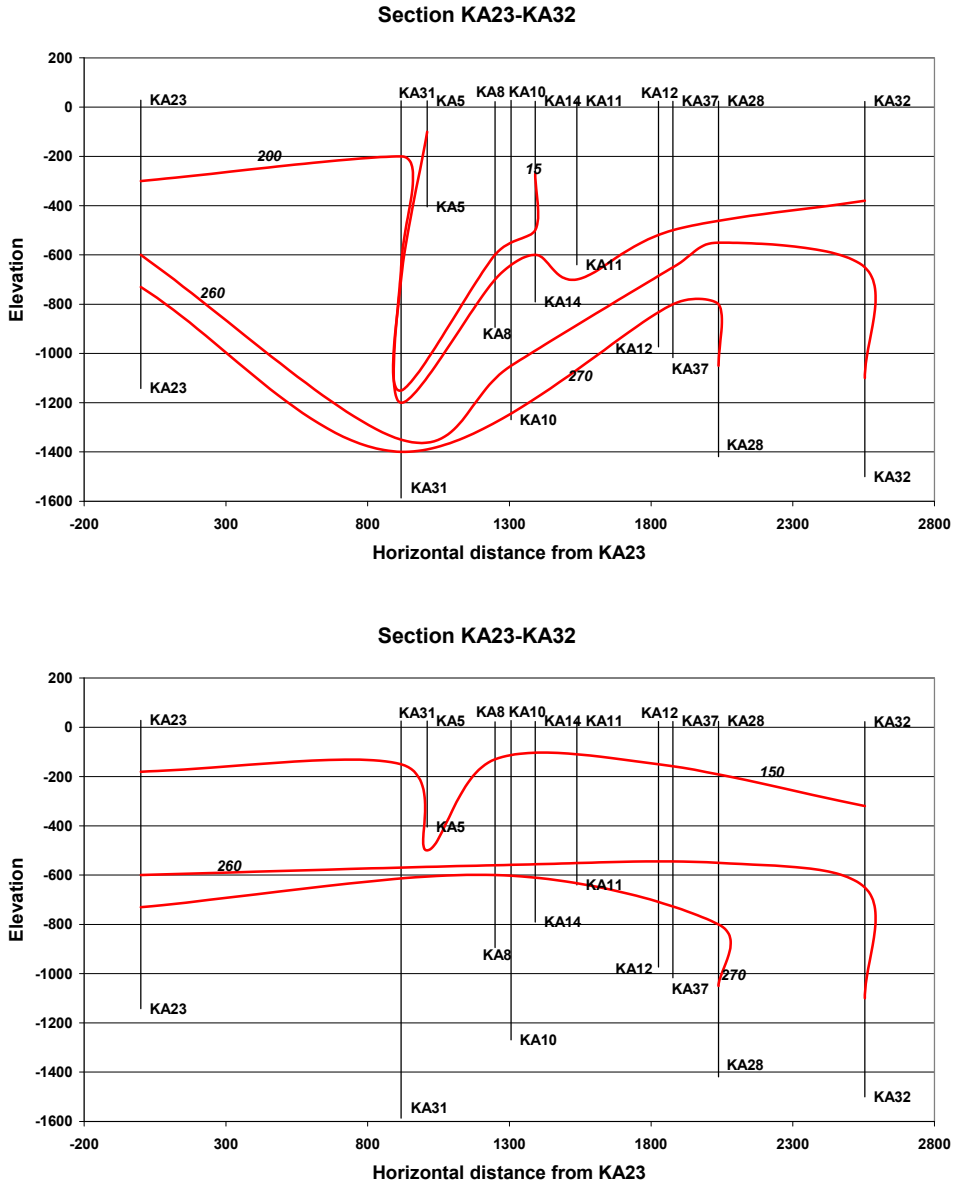

FIGURE 70: Isothermal section SW-NE. Above original temperatures, below temperatures in 1985

4. PHASE 4 – MAINTENANCE

In the early 1980s, New Zealand underwent extensive restructuring and financial reforms. This had implications for Kawerau. The steam field remained in government ownership but was now run strictly as a service for the mill, and expected to be profitable. Some makeup wells were needed because of cooling and deposition, so KA21, 27, 28 & 35 were connected. There were a number of significant changes:

- Reservoir modelling started
- Shallow injection was used for some waste water
- Tracer tests were carried out
- Antiscalant was tried and then adopted.

Figure 71 shows the production history up to the end of this period.

One interesting event during this period was the Edgecumbe earthquake. A major fault passing through the field moved, with significant displacement. There was apparently no effect on the field.

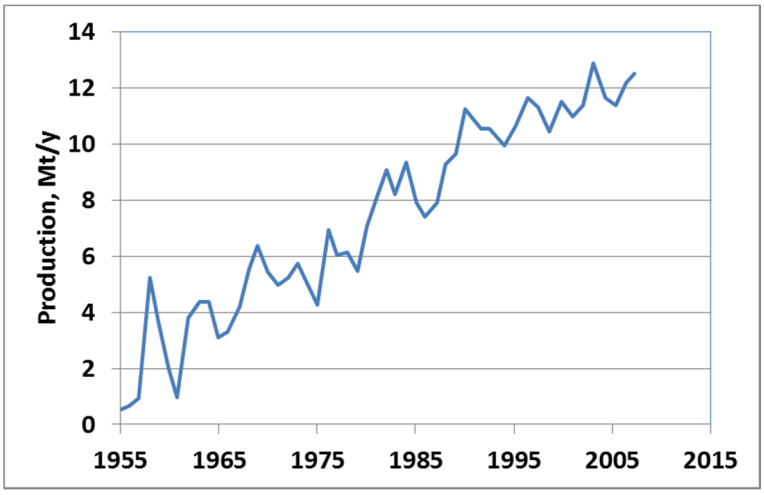

FIGURE 71: Production history to 2005 (Wigley 1993)

5. PHASE 5 – EXPANSION

In the 2000s further reforms had further impact on Kawerau. There was a treaty settlement (claim by indigenous Maori) which included the transfer of most of the existing wellfield to Ngati Tuwharetoa, who continued to run it to supply steam to the mill, but were keen for other expansion. Reform of the electricity market meant that the monopoly NZ Electricity was broken up and generation was open to any party. One landowner in the field whose land included a well (KA24) developed a small power station using the well. Mighty River Power, through a subsidiary Kawerau Geothermal Limited, developed a 110 MW power station. Figures 72 and 73 show the wellfield in 2008. The background photo is from 2005 and does not include the power station.

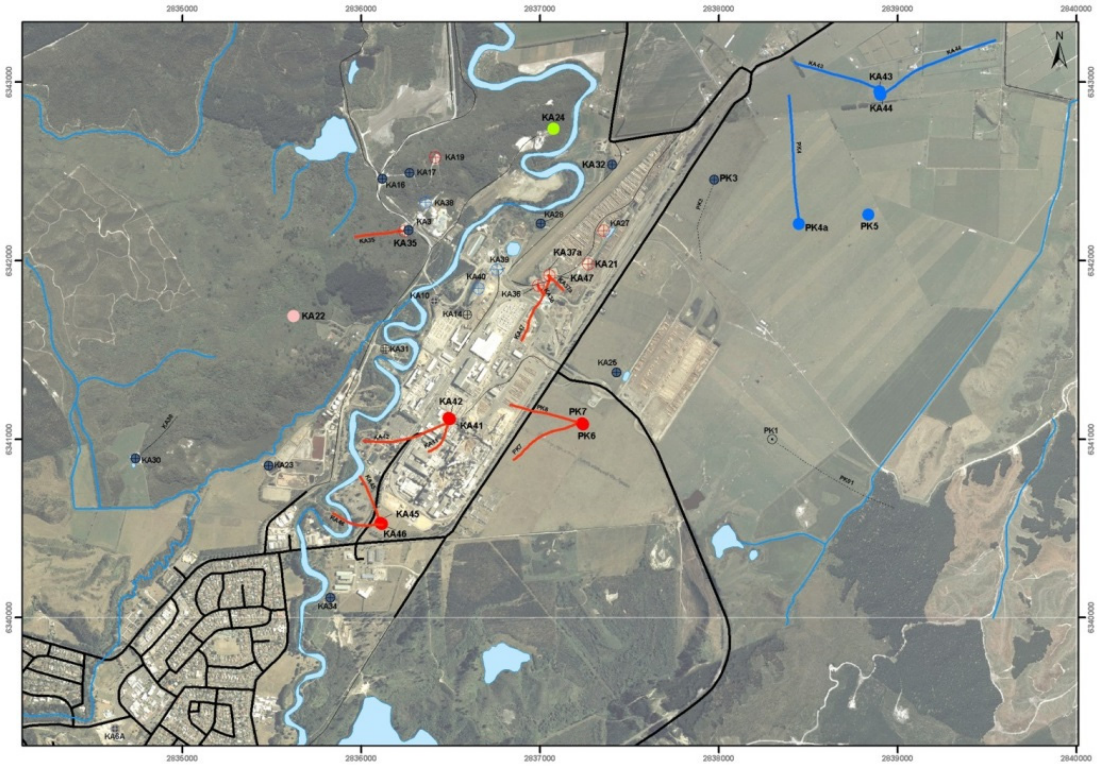

FIGURE 72: Wellfield in 2008

Land access is now a significant issue. In the 1950s-1980s, the government program could drill on any land, and did so. (The long-term consequence of drilling on someone else's land has been that the well ultimately became the property of the landowner.) Now the landowner's agreement is required. Much of the land in the field is owned or controlled by the mill, but the rest is in a variety of parcels. Further,

much of the field is occupied by the mill, with the addition of another mill making tissue, and all their infrastructure. This creates significant restrictions in drilling and locating pipelines.

The presence of multiple developers, and other potential developers, has created sensitivity about information. The reservoir model in particular is guarded carefully although all developers have access to it.

There was more drilling, with wide diameter production wells being drilled and Kawerau again had the largest wells in NZ inKA46 & 47.

The field is now managed differently from past developments:

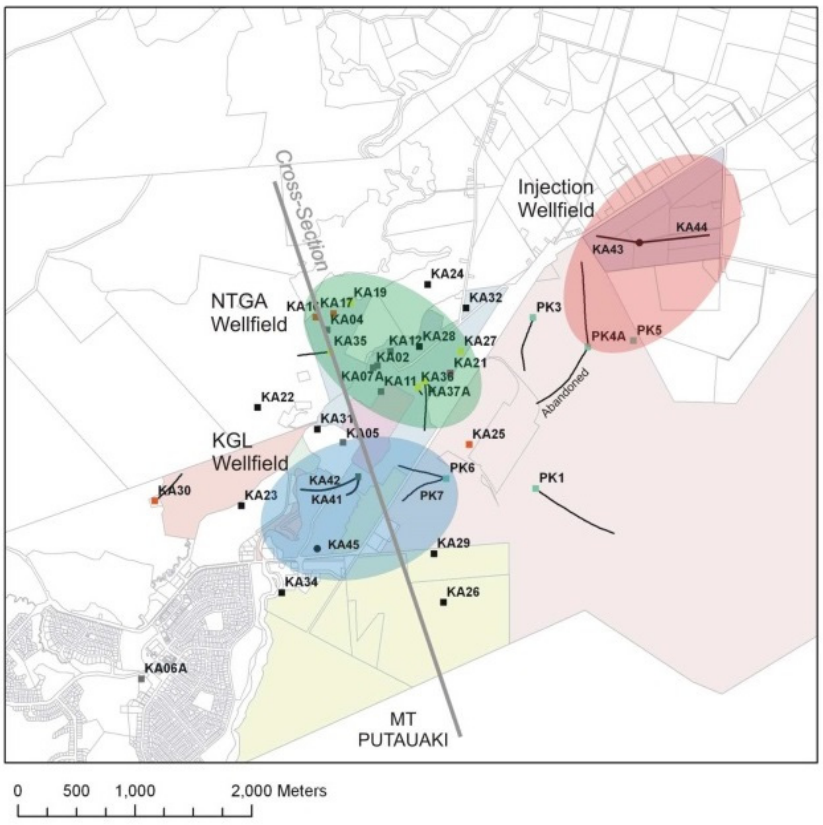

FIGURE 73: Wellfield in 2008

- All new developments have full injection
- Injection is deep and peripheral
- Production wells all now produce from greywacke which is now regarded as the main reservoir rock
- There is extensive interference testing
- The resource capacity is defined by the simulation model which has been progressively updated and recalibrated
- The resource is not well defined by Schlumberger resistivity
- The upflow has still not been drilled!

The recent resistivity, shown in Figure 68, outlines a large field with all development on the western side. Drilling has established that the eastern part of the field is hot (~200°C) but with poor permeability.

Figure 74 shows the current conceptual model. The basement rock is greywacke. It is overlain by volcanics with a complicated pattern of buried and exposed rhyolite domes. The upflow originates in the south-east, at depth in the greywacke. The best permeability is also found in the upper greywacke. The upflow lies in the south, under Mt Putauaki. However the volcano is not the field source, because the field is over 200,000 years old but the volcano is only 5,000 years old.

Figure 75 shows the production history to 2010, with the consented totals also shown. Two consents have recently been issued but have yet to be much used. Some of the increase planned is for more generation and some for expanded direct heat uses. Since 1985 when consents were first required, production has been less than consented because it is limited to demand.

The expansions have been justified by the simulation model.

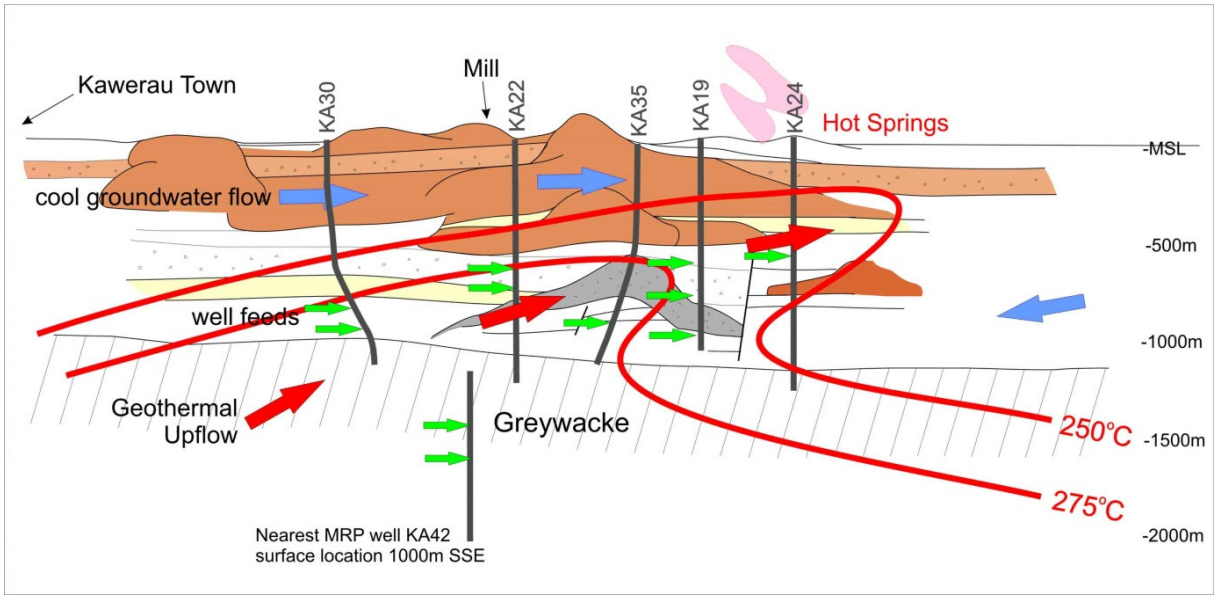

FIGURE 74: Kawerau conceptual model

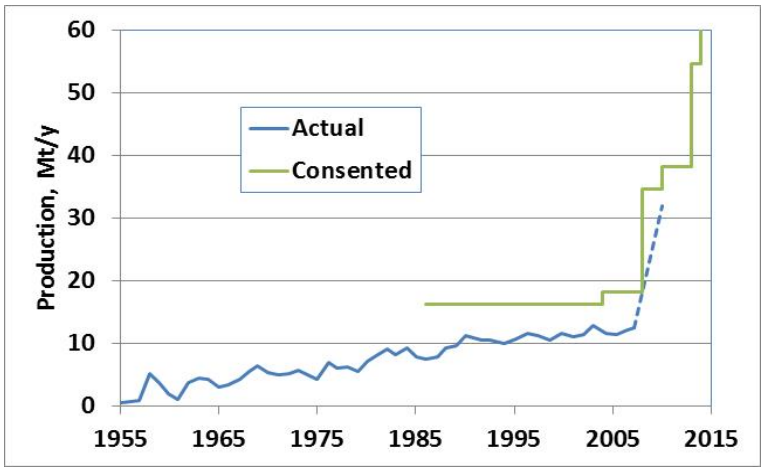

FIGURE 75: Production history and consented production

The upflow lies to the south of the existing wellfield – all existing production wells, unless shallow, encounter a reversal at depth. Two wells have been drilled here in the past but went to only 1000m. When more production is needed it is planned to expand the wellfield southwards.

Reservoir management at Kawerau has had some distinctive features:

- Because field was allocated to the mill, resource capacity was not an issue and little effort was put into it until recently;
- Conventional resistivity not very helpful;
- Critical issues for management were cold water invasion and later deposition, both identified quickly although cold water not quantified until 2000s.

REFERENCES

Apuada, N.A., Sigurjonsson, G.F., & Oanes, A.F., 2010 "Evaluation of the hydrothermal system of Biliran Island, Philippines" WGC paper 0618

Barelli, A., Cei, M., Lovari, F., & Romangoli, P., 2010b "Numerical modelling for the Larderello-Travale geothermal system (Italy)" World Geothermal Congress paper 2225

Belen, R.Jr., Aunzo, ., Strobel, C., & Mogen, P., 1999 "Reservoir pressure estimation using PTS data" Proc., 24th Workshop on geothermal reservoir engineering, Stanford University

Bloomer, A., 2011 "Kawerau direct heat use: historical patterns and recent developments" Proc., NZ Geothermal workshop paper 75

BoPRC, various: Consent decisions

Clotworthy, A., 2008 "Ohaaki field management" presentation to NZGA seminar

Davarzani, J., & Roesner, R.E., "Surveying steam injection wells using production logging instruments" Transactions, Geothermal Resources Council, v9pt1 pp451-456

Desormier, W.L.,1987 "Dixie Valley six well flow test" Transactions, Geothermal Resources Council, v11

Faulds, J., Coolbaugh, M., Bouchot, V., Moeck, I., & Oğuz, K., 2010 "Characterising structural controls of geothermal reservoirs in the Great Basin, USA and Western Turkey: Developing successful exploration strategies in extended terranes" WGC paper 1163

Grant, M.A., 1987 "Reservoir engineering of Wairakei geothermal field" in "Geothermal Reservoir Engineering" NATO Advanced Study Institute, ed. Okandan

Grant, M.A., 1987 "Reservoir physics and conceptual modelling" in "Geothermal Reservoir Engineering" NATO Advanced Study Institute, ed. Okandan.

Grant, M.A., 2008 "Decision tree analysis of possible drilling outcomes to optimise drilling decisions" Proc 33rd Workshop on Geothermal Reservoir Engineering, Stanford University.

Grant, M. A., & Bixley, P. F., 1995 "An improved algorithm for spinner profile analysis" Proc., NZ Geothermal Workshop, Auckland University

Grant, M.A., Bixley, P.F., & Wilson, D.W., 2006 "Spinner data analysis to estimate wellbore size and fluid velocity" Proc 28th NZ Geothermal Workshop

Grant, M.A., & McGuinness, M., 1985 "Hydrology" in DSIR 1985 "Ngawha investigation report"

Grant, M.A., Powell, T., & Spinks, K., 2008 "Kawerau geothermal field" Paper presented at NZGA/WPRB workshop

Grant, M.A. & Wilson, D., 2007 "Interference testing at Kawerau 2006-2007" Proc 29th NZ Geothermal Workshop

Gunnarson, G., Arnaldsson, A., & Oddsdóttir, A.L., 2010 "Model simulations of the geothermal fields in the Hengill area, south-west Iceland" World Geothermal Congress paper 2251

Guo, G., Axelsson, G., Chao, Y., & Baodong, X., 2010 "Assessment of the Hofsstadir geothermal field, W-Iceland, by lumped parameter modelling, Monte Carlo simulation and tracer test analysis" World Geothermal Congress paper 2209

Hadi, D.K., Sugandhi, A., Roberts, J.W., & Martiady, K., 2010 "Utilizing vertical discharge tests as an effective means for well decision making at the Darajat geothermal field, Indonesia" World Geothermal Congress, paper 2280

Heiberg, S.J., Bixley, P.F., & Lee, S.G., 2011 "Successful acid treatment of a production well in the Tauhara field, New Zealand" Proc., 33rd NZ geothermal workshop

Hino, T., Itoi, R., Tanaka, T., Pambudi, N.A., & Khasani, 2013 "Natural state modelling of geothermal reservoir at Dieng, central Java, Indonesia" Transactions, Geothermal Resources Council, v37, pp831-835

Jun, L., & Dan, L., 2005 "Reservoir evaluation of the Zhouliangzhuang geothermal field, Tianjin, China" WGC paper 1154

Kamah, M.Y., Dwikorianto, T., Zuhro, A.A., Sunaryo, D., & Hasibuan, A., 2005 "The productive feed zones identified based on spinner data and application in the reservoir potential review of Kamojang geothermal area, Indonesia" WGC paper 1111

Kipyego, E., O'Sullivan J.., & O'Sullivan, M., 2013 "An initial resource assessment of the Menegai caldera geothermal system using and air-water TOUGH2 model" Proc 35th NZ geothermal workshop.

Lim, Y.W., Grant. M., Brown, K., Siega, C., & Siega, R., 2011 "Acidising case study – Kawerau injection wells" Proc 36th Workshop on Geothermal Reservoir Engineering, Stanford University

Lutz., S.J., Walters, >, Pisotone, S., & Moore, J.N., 2012 "New insights into the High-temperature reservoir, Northwest Geysers" Transactions, Geothermal Resources Council, v36

Malate, R.C., 2008 "Management of geothermal resource: PNOC-EDC experience" presentation to NZGA seminar

McCabe, W.J., Manning, M.R., & Barry, B.J., 1980 "Tracer tests Wairakei" Institute of Nuclear Sciences report INS-R—275

McNitt, J.R., 1995 "A new model for geothermal exploration of non-volcanic systems in extended terrains" WGC pp1115-1118

McNitt, J.R., Robertson-Tait, A., Klein, C.W., & Sanyal, S.K., 1988 "An integrated approach to conceptual modelling of geothermal reservoirs" Japan International Geothermal Symposium

Menzies, A.J., Swanson, R.J., & Stimac, J.A., 2007 "Design issues for deep geothermal wells in the Bulalo geothermal field, Philippines" Transactions, Geothermal Resources Council v31, pp251-256

Menzies, T., 2013 "Well testing program to determine well and reservoir characteristics" ITB geothermal workshop, Bandung

Menzies, A.J., Villaseñor, L.B., & Sunio, E.G., 2010 "Tiwi geothermal field, Phil;ippines: 30 years of commercial operation" WGC paper 0648

O'Sullivan, M.J., Pruess, K., & Lippmann, M.J., 2001 "State of the art of geothermal reservoir simulation" Geothermics 30, pp395-429

O'Sullivan, M.J., Yeh, A., & Mannington, W.I., 2009 "A history of numerical modelling of Wairakei geothermal field" Geothermics 38, pp155-168

Osborn, W.L., & Spielman, P., 1995 "Measurement of velocity profiles in production wells using wireline spinner surveys and rhodamine WT fluorescent tracer; Coso geothermal field (California)" Trans., Geothermal Resources Council v19 pp521-528

Porras, E.A., & Bjornsson, G., 2010 "The Momotombo reservoir performance upon 27 years of exploitation" WGC paper 0638

Rae, A.,2013 "Geothermal systems and modelling" presentation to NZGA seminar

Serpen, U., & Satman, A., 2000 "Reassessment of the Kizildere geothermal reservoir" WGC paper 0696

Siega, C., Grant, M.A., & Powell, T., 2009 "Enhancing injection well performance by cold water stimulation in Rotokawa and Kawerau geothermal fields" Proc., PNOC-EDC Conference

Stevens, L., 2000 "Pressure, temperature and flow logging in geothermal wells" WGC paper 0254

Tosha, T., Ishido, T., & Sugihara, M., 2010 "Self-potential monitoring with reservoir simulation in a geothermal field, Japan" WGC paper 1385

Wallis, I.C., McNamara, D., Rowland, J.V., & Massiot, C., 2012 "The nature of fracture permeability in the basement greywacke at Kawerau geothermal field, New Zealand" Proc., Stanford geothermal workshop

White, P., Mackenzie, K., Brotheridge, J., Seastres, J., Lovelock, B., & Gomez, M., 2012 "Drilling confirmation of the Casita indicated geothermal resource, Nicaragua" Proc., 34th NZ geothermal workshop

Wigley, D.M., & Stevens, L., 1993 "Developments in Kawerau geothermal field" Proc., NZ Geothermal workshop, pp47-53

Wisian, K., Blackwell, D.D., & Benoit, D., 1998 "Thermal conditions in Beowawe well Ginn 2-13" Transactions, Geothermal Resources Council, v22 pp561-565

Wissan, K.W., 2000 "Insights into extensional geothermal systems from numerical modelling" WGC paper 0572

Zarrouk, S.J., & Ratouis, T.M.P., 2013 "Factors controlling large-scale convective geothermal system in the Taupo Volcanic Zone (TVZ), New Zealand" Proc 35th NZ geothermal workshop.

Zúñiga, S.C., 2005 "Transmissivity *(kh)* determination in the Miravalles geothermal field" WGC paper 1108